

Heliophysics Senior Review 2013

The Reuven Ramaty High Energy Solar Spectroscopic Imager (RHESSI)

Samuel Krucker, Principal Investigator

Brian Dennis, Mission Scientist

Manfred Bester, Director of Operations

Laura Peticolas, E/PO Manager

Table of Contents

Executive Summary	1
1 Science and Science Implementation	2
1.1 <i>The First 11 Years</i>	2
1.2 <i>Prioritized Science Goals (PSGs) - Progress to Date</i>	3
1.2.1 Science Goal 1 – Evolution of Solar Eruptive Events (SEEs).....	3
1.2.2 Science Goal 2 – Flare-accelerated Electrons.....	7
1.2.3 Science Goal 3 – Flare-accelerated Ions.....	9
1.2.4 Science Goal 4 – Flare-heated Plasma.....	12
1.2.5 Science Goal 5 – Global Structure of the Photosphere	15
1.2.6 Science Goal 6 – Nonsolar Objectives	16
1.3 <i>How the Prioritized Science Goals will be achieved</i>	17
1.3.1 Science Goal 1 – Evolution of Solar Eruptive Events	17
1.3.2 Science Goal 2 – Flare-accelerated Electrons.....	18
1.3.3 Science Goal 3 – Flare-accelerated Ions.....	19
1.3.4 Science Goal 4 – Flare-heated Plasma.....	20
1.3.5 Science Goal 5 – Global Structure of the Photosphere	20
1.3.6 Science Goal 6 – Nonsolar Objectives	21
1.4 <i>Potential for Performance in the FY-14 to FY-18 timeframe</i>	21
1.4.1 Relevance to the SMD Science Plan and contributions to HSO.....	21
1.4.2 Productivity and Vitality of Science Team	21
1.4.3 Data Accessibility and Usability	22
1.4.4 Promise of future impact and productivity	24
2 TECHNICAL and BUDGET	24
2.1 <i>Spacecraft</i>	24
2.2 <i>Instruments</i>	25
2.2.1 Spectrometer and Cryocooler	25
2.2.2 Imager	27
2.2.3 Aspect System	27
2.3 <i>Ground System</i>	27
2.3.1 Ground Stations	28
2.3.2 Mission Operations Center.....	28
2.3.3 Science Operations Center	28
2.4 <i>References</i>	29
Appendices	30
3 Education and Public Outreach	30
3.1 <i>UC Berkeley Budget</i>	35
3.2 <i>Goddard Budget (in \$K)</i>	35
4 RHESSI Legacy Mission Archive Plan	36
4.1 <i>Introduction</i>	36

4.2	<i>Current RHESSI Data Archive, Software and Documentation</i>	36
4.2.1	RHESSI Data Archive	36
4.2.2	Software	37
4.2.3	Documentation and Support.....	37
4.3	<i>Plans for the RHESSI Legacy Archive</i>	38
4.3.1	Introduction	38
4.3.2	Data Products	38
4.3.3	Analysis Tools for Level-0 data	41
4.3.4	Documentation	41
4.3.5	Distribution.....	41
4.3.6	Schedule	42
4.4	<i>References</i>	42
Acronym List		45

EXECUTIVE SUMMARY

RHESSI has been providing unique diagnostic observations of high-energy processes in solar flares for over 11 years. These observations address the key Heliophysics goal of understanding the fundamental processes of particle acceleration and energy release in solar eruptions, both flares and coronal mass ejections (CMEs). The resulting photon emissions and accelerated particles directly affect our Home in Space, and are especially important for our Journey Outward.

RHESSI is designed for imaging spectroscopy of hard X-ray (HXR) and gamma-ray continua emitted by energetic electrons, and gamma-ray lines produced by energetic ions. The single instrument makes imaging and spectroscopy measurements with a few arcsecond angular resolution and one- to a few- keV energy resolution at energies from soft X-rays to gamma-rays (3 keV - 17 MeV). **No other current or planned observatory has this ability to provide direct quantitative information on the energetic electrons and ions that carry such a predominant part of the released energy in a flare.**

RHESSI was launched in February 2002, and has operated successfully ever since. Over 70,000 events are included in the RHESSI Flare List, over 14,000 of them with detectable emission above 12 keV, and 35 above 300 keV. Twenty-seven events show gamma-ray line emission. All the data and the analysis software have been made immediately available to the scientific community. This has resulted in **over 1,000 refereed papers** published to date that utilize RHESSI observations, with **over 200 in the three years since the last Senior Review** and a total of well over **1,000 citations per year**.

The value of future RHESSI observations is now greatly enhanced by improved complementary observations compared with those available during the first eight years of RHESSI's operational lifetime. Groundbreaking observations of thermal plasmas, magnetic fields, and heliospheric effects are now being provided on a regular basis by instruments on the Solar Dynamics Observatory (SDO), Hinode, STEREO, and other components of the Heliophysics System Observatory (HSO), and instruments on the Fermi astrophysics mission are providing X-ray and gamma-ray spectroscopy (limited imaging and modest energy resolution) from ~10 keV to GeV energies. New and upgraded ground-based radio and optical facilities, such as the Expanded Owens Valley Solar Array (EOVSA), are becoming available to provide microwave imaging spectroscopy data that give a complementary perspective on the energetic electrons and heated plasma deduced from RHESSI's X-ray observations.

No other instrument currently operating or scheduled for flight can provide high-resolution X-ray and gamma-ray imaging spectroscopy data that are essential to so many studies of the active Sun. Thus, **RHESSI remains an essential component of HSO**. Interpretation of data from RHESSI, especially in conjunction with data from other instruments, forms a key part of *“developing a comprehensive scientific understanding of the fundamental physical processes that control our space environment and that influence our Earth's atmosphere.”*

The RHESSI spacecraft and instrument continue to operate well. The mission has no expendables and reentry is not predicted to occur until 2018 at the very earliest. The germanium detectors have been annealed three times, most recently in February 2012, to remove most of the effects of radiation damage, including degradation in energy resolution and loss of active volume. Future anneals may result in detector desegmentation but we nevertheless expect that RHESSI's core hard X-ray imaging spectroscopy capability can be maintained into 2018.

1 SCIENCE AND SCIENCE IMPLEMENTATION

1.1 The First 11 Years

After over eleven years of near-continuous operation, RHESSI (Lin et al. 2002) continues to provide unique high-resolution X-ray and gamma-ray imaging spectroscopy observations over the range of energies from 3 keV to 17 MeV, with high spatial resolution (down to 2 arcseconds), spectral resolution (as fine as 1 keV FWHM), and time resolution (as fine as 2 s for imaging and <1 s for spatially-integrated flux measurements). This range covers soft X-rays emitted by hot thermal plasma, hard X-ray and gamma-ray bremsstrahlung continuum emitted by energetic electrons, and nuclear gamma-ray lines produced by energetic ions. Since the various X-ray and gamma-ray emission processes involved are quantitatively well-understood, the properties of the thermal plasma and the emitting electrons and ions (their spectra, fluxes, and locations) can be directly and quantitatively determined.

A detailed description of the RHESSI mission, instrument, and software is given in the first six papers of the Nov. 2002 issue of *Solar Physics* (210, pp. 3-124); we here provide a brief summary. The RHESSI imager is made up of nine Rotating Modulation Collimators (RMCs), each consisting of a pair of widely separated parallel grids mounted on the rotating spacecraft. The pitches, thicknesses, and separations of the various grids allow images to be reconstructed up to gamma-ray energies with angular resolutions as fine as ~2 arcseconds. Behind each RMC is a segmented germanium detector (GeD), cooled by a mechanical cryocooler, to detect photons from 3 keV to 17 MeV with high spectral resolution (~1 to 10 keV FWHM). An automated shutter system allows a wide dynamic range (~ 10^6) of flare intensities to be handled with high sensitivity to microflares and minimal pulse pile-up during large X-class flares.

As the spacecraft rotates, the RMCs convert spatial information from the source into temporal modulation of the photon counting rates in the GeDs. Sub-arcsecond pointing information is provided by the Solar Aspect System (SAS) and two redundant Roll Angle Systems (RAS). The spin-stabilized (~15 rpm) spacecraft is Sun-pointing to within ~0.2° and operates autonomously. The energy loss and time of arrival for every photon recorded by the GeDs are stored in a solid-state memory (sized to handle the largest flare) and telemetered to the ground during passes over Berkeley, Wallops, or, on occasion, other ground stations.

RHESSI observations reveal that the flare-accelerated electrons and ions are both intimately related to the magnetic restructuring associated with solar eruptive events (SEEs), and that together they can contain a large fraction of the total released energy. There have been systematic studies of extended coronal HXR sources and of the relatively weak coronal HXR emission visible to RHESSI when the flare footpoints are occulted by the limb. As a result of these studies, fundamental new information has been obtained on the location and physical characteristics of the energy release and electron and ion acceleration regions.

RHESSI has also made fundamental discoveries in other areas of solar, terrestrial, and astrophysical studies. The extended solar minimum in 2008 and 2009 was an ideal time to exploit RHESSI's uniquely high sensitivity from ~3 to 15 keV for systematic studies of microflares and their implications for coronal heating. RHESSI's solar aspect system (SAS) has provided the best global measurements of the large-scale structure of the solar photosphere (e.g., the solar oblateness) ever obtained, opening up new areas of research that relate to the nature of the solar cycle now and in the future. RHESSI's discovery that Terrestrial Gamma-Ray Flashes (TGFs) commonly extend up to >~20 MeV has revitalized the study of these lightning-related high-energy phenomena. RHESSI also provides unique measurements of astrophysical high-energy phenomena such as magnetars and cosmic gamma-ray bursts.

One of the greatest strengths of the RHESSI observations lies in their complementarity with data sets from other instruments in the HSO. The relationship between RHESSI and SDO,

STEREO, Hinode, etc. is symbiotic. These other missions provide vital context information for the interpretation of RHESSI high-energy observations. For example, to understand what is special about the flare and CME-related particle acceleration and energy release regions identified by RHESSI, we need good magnetic field models based on accurate photospheric (and chromospheric, if available) measurements, and information on the magnetic topology, waves, shocks, and ambient conditions in the corona obtained by instruments on Hinode, STEREO, and SDO, as well as ground-based optical and radio observatories. Of equal importance, RHESSI data also provide a vital complement to studies with primary basis in other observations. Studies of the physical conditions in active regions, for example, are anchored by RHESSI's ability to probe the spatial structure of the flare energy dissipation through high-resolution imaging spectroscopy of HXRs.

At present, we are near the maximum phase of Solar Cycle 24, and RHESSI has been detecting an average of ~5 flares per day at energies above 12 keV since 2011. Useful average rates above one such flare per day should persist through 2017. For the first time, we will have a full complement of multi-platform solar and heliospheric measurements throughout a full cycle. We can expect synergistic studies of many SEEs in the coming years using the array of instruments in the HSO, allowing for a much more insightful analysis than was possible through much of RHESSI's observations during the previous solar cycle. Historical records of activity show that major energetic events can occur at almost any phase of the solar cycle and, furthermore, that the aspects of solar activity revealed in flare/microflare occurrence patterns may help us to understand the cycle itself.

1.2 Prioritized Science Goals (PSGs) - Progress to Date

RHESSI's design was optimized for its primary science goal of understanding solar flare energy release and particle acceleration. This goal can be broken down into the following four major components, each related directly to the basic mechanisms of magnetic-energy conversion: (1) the evolution of SEEs, (2) the acceleration of electrons, (3) the acceleration of ions, and (4) the origin of the thermal plasma. Our prioritization of the science goals is based on the relative frequencies of events and the potential scientific return in each case. These solar flare goals are followed in our PSG list by other scientific objectives derived from RHESSI's serendipitous capabilities for making scientifically important observations of (5) the optical Sun and (6) X-ray and gamma-ray sources of both terrestrial and astrophysical origin. For each of these six goals, we outline the current status and describe the important progress that has been made to date. In Section 1.3, we discuss how new observations made with RHESSI and other space- and ground-based instruments in the coming years can achieve these goals.

1.2.1 Science Goal 1 – Evolution of Solar Eruptive Events (SEEs)

A primary goal of heliophysics is to understand the origin and evolution of solar flares and coronal mass ejections, and the relationship between them. It is now well established that magnetic reconnection in the corona plays a central role in the physics of solar eruptive events (SEEs), explosions in which a flare and a CME are observed together. Recent RHESSI observations, especially combined with SDO/AIA and radio imaging observations, are now elucidating how these events are driven and how they evolve.

1.2.1.1 *The Primary Reconnection Current Sheet*

Direct visual evidence for magnetic reconnection in a SEE has recently been obtained for a C2.3 flare that occurred on 2011 August 17 (Su et al. 2013; see also Liu et al. 2013). This is best seen in the AIA 131-Å videos in association with RHESSI X-ray images available at <http://hesperia.gsfc.nasa.gov/hessi/movies/17Aug2011>. Two stills from one of these videos, with overlaid RHESSI X-ray contours, are shown in Figure 1-1.

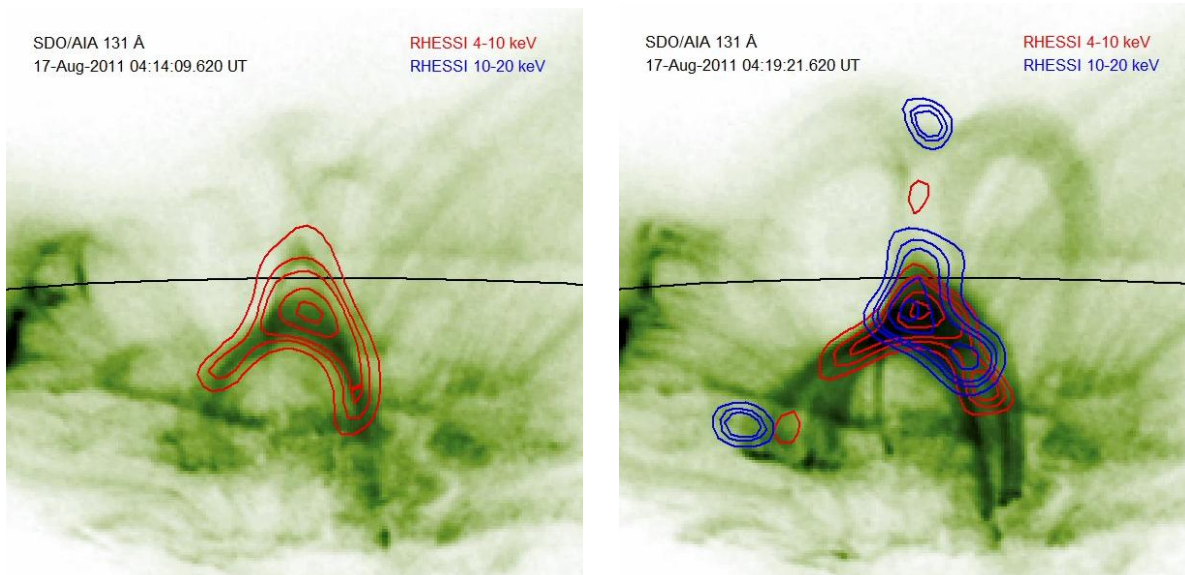


Figure 1-1. Stills for two different times from SDO/AIA 131-Å movie of flare on 2011 August 17 illustrating the power of complementary AIA and RHESSI observations.

The left picture shows the situation near the start of the event. The 131-Å image shows the X-point just beginning to separate into two Y-points. Hot loops below are seen in both EUV and X-rays at 4–10 keV. In the right picture, about 5 minutes later, the two Y-points have separated by tens of arcseconds. HXR sources at 10-20 keV are visible both above and below the presumed current sheet between them (and also at one footpoint). Two patches of thermal X-ray emission (4-10 keV) are also visible in the corona, one from the top of flare arcade loops seen in the AIA image and the second from a compact region above the loop-top sources. Such double coronal sources seen in similar events were previously identified with the lower and upper jets associated with magnetic reconnection occurring between them (see Holman 2012a).

The AIA video shows the lateral development of the flare arcade. The reconnection begins at one end of the sheared arcade and propagates along the arcade (in this case, toward the observer). This process generates both an arcade of hot flare loops below the laterally expanding current sheet and the magnetic flux rope above it. The latter forms the core of the subsequent CME. Observations made with RHESSI, white-light coronagraphs, and other instruments have demonstrated that, once fully formed, the current sheet expands upward with the erupting CME.

Liu et al. (2013) reported similar SDO/AIA and RHESSI observations of a limb event that occurred in 2012. Height-time diagrams derived from AIA 131Å videos show the gradual evolution of the flare loop tops and the reconnection region as well as the evolution of the jets from the reconnection region. Comparisons with the location and spectrum of the RHESSI hard X-ray emission support previous indications (e.g., Holman 2012a) that electrons are primarily accelerated in the reconnection jets, not in the reconnection current sheet itself.

1.2.1.2 *Breakout Reconnection*

In order for a newly-formed magnetic flux rope to propagate outward to become a CME, it must interact with the overlying magnetic field. If the CME has a field component opposite to that of the overlying field, it can escape by reconnecting with this field. Such a breakout reconnection scenario is included in many numerical simulations of SEEs, but observational support for it has so far been weak. Strong evidence for breakout reconnection has recently been identified in the combined meter-wave radio and RHESSI X-ray observations of a SEE

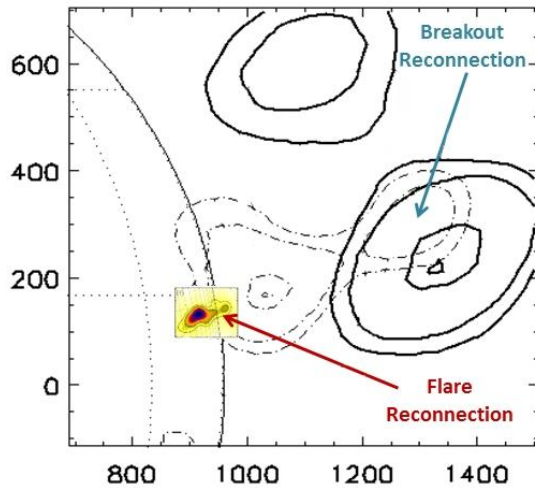


Figure 1-2. Evidence for breakout reconnection in the 2003 November 3 SEE from radio and X-ray data. Contours show radio sources at 432 MHz (dot-dash) and 236 MHz (solid black). The color insert shows RHESSI 15 – 20 keV sources.

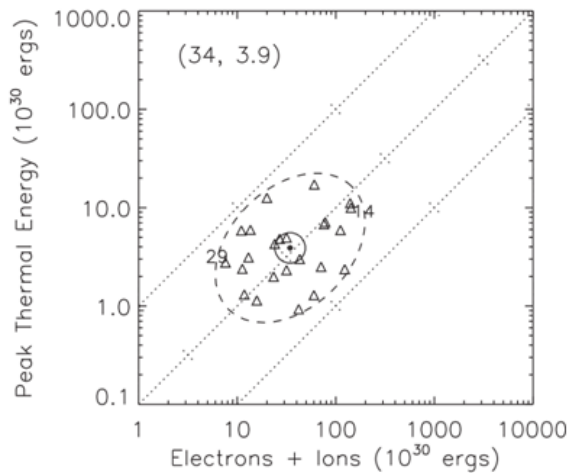


Figure 1-3. Scatter plot showing that the peak thermal energy is, on average, about an order of magnitude smaller than the time-integrated energy in flare-accelerated particles (Emslie et al. 2012).

shown in Figure 1-2 (Aurass et al. 2013). The two observed coronal X-ray sources serve to locate the two jets above and below the indicated flare reconnection site. Two radio sources located radially above the X-ray sources were imaged at 432 MHz with the Nançay and the AIP (Potsdam) Radiospectrographs. The upper of these two 432 MHz sources was flanked by two sources at 236 MHz along a line perpendicular to the radial line through the X-ray and 432 MHz sources. The most plausible explanation for this arrangement is that the lower 432 MHz source, like the upper X-ray source, was associated with the upward-directed flare reconnection jet. The upper 432 MHz source, which remained stationary, was associated with breakout reconnection ahead of the developing magnetic flux rope. The two 236 MHz sources would then naturally be associated with the roughly horizontal jets from the breakout reconnection well above the flaring active region.

1.2.1.3 *SEE Global Energy Budget*

In a series of papers, Emslie et al. (2004, 2005, 2012) used observations from a wide variety of spacecraft to study the partition of energy from a SEE into various energetic components. These include “primary” components such as accelerated electrons and ions, “intermediate” products such as heated thermal plasma, and “final” products such as radiated energy, CME kinetic energy, and energy in solar energetic particles (SEPs). Studying the ratios of these energetic components gives valuable clues as to the nature of the energy release and particle acceleration processes. An example of such a comparison, derived primarily from RHESSI observations, is shown in Figure 1-3. It shows that only some 10% of the energy initially released as accelerated electrons and ions subsequently manifests itself as energy in

hot thermal plasma. Other comparisons, for the same set of events, show that a large fraction of the magnetic energy released in a SEE is manifested as accelerated electrons and ions, and that, to within an order of magnitude, there is a general equipartition between the flare and the CME energies in an SEE.

1.2.1.4 *Flare Energy Release and CME Acceleration*

Given the geoeffectiveness of CMEs, the effort to understand and eventually to predict these powerful solar events has become a major activity of the Heliophysics program. Infrequently, CMEs can occur in the absence of flares, but fast and powerful CMEs tend to be

associated with the most energetic flares. Most models of these events include an intimate magnetic connection between the initiation and early acceleration of the CME and the energy release in the associated flare. Berkebille-Stoiser et al. (2012) studied the initial dynamics of a set of CMEs observed with STEREO/EUVI and COR1 in comparison with the energy release and particle acceleration in the associated flares inferred from RHESSI. Figure 1-4 shows that the CME acceleration profile is highly synchronized with the flare energy release rate and tightly correlated with the accelerated electron spectra in the associated flares. Particularly good correlations are obtained between the peak acceleration and initiation height of the CMEs with the spectral index of the flare-accelerated electrons, implying that CMEs erupting at low coronal heights, i.e., in regions of stronger magnetic fields, are accompanied by flares which are more efficient at accelerating electrons to high energies.

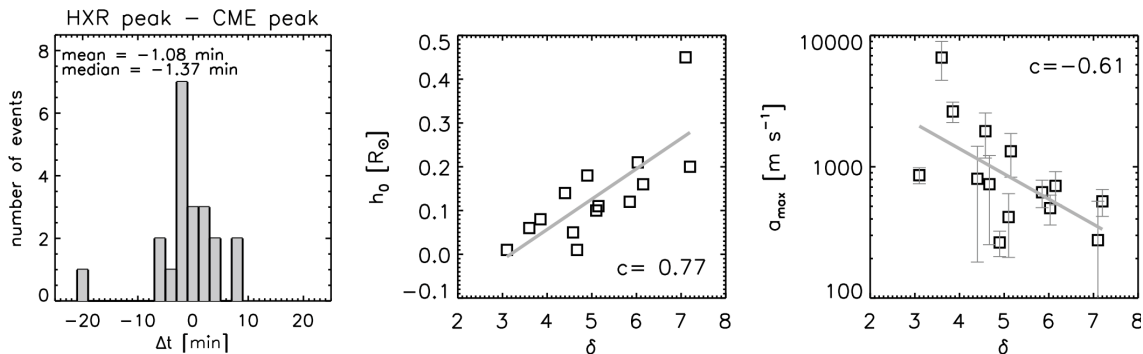


Figure 1-4. Distribution of the time lags between the peak of the flare HXR emission and the peak of the impulsive CME acceleration (left). Scatter plot of the CME initiation height (middle) and CME peak acceleration (right) against the spectral index of the accelerated electron spectrum derived from RHESSI flare observations. Adapted from Berkebille-Stoiser et al. (2012).

1.2.1.5 Flares, CMEs, and SEPs

HXR emission directly from CMEs

Statistical studies of RHESSI observations of nonthermal HXR emission from electrons injected upward from the acceleration site into the escaping CME have shown that this rarely-observed phenomenon actually describes a general feature of fast CMEs (e.g., Krucker et al. 2008a). Such coronal HXR sources are generally difficult to observe because of the relatively low density of the CME (Krucker et al. 2007) and the usual presence of intense footpoint sources. Hence, these events are best seen in highly occulted events where the main flare emissions occur behind the solar disk. However, some extremely bright events exist where the emission is seen from disk events as well (Bain & Fletcher 2009). The injection into the CME core is observed to be simultaneous with the injection into the footpoints, and it can occur into very large structures of up to >300 arcsec in extent. Quantitative comparisons with SDO/AIA images suggest that the nonthermal electrons heat the core of the ejected CME material making the core visible in the hot AIA channels, particularly the $131\ \text{\AA}$ channel (see Figure 1-5, taken from Glesener et al. 2013). Hence, the previously unexplained heating observed in CME material as it moves outward (e.g., Landi et al. 2010) is, at least for some events, due to flare-accelerated nonthermal electrons appearing in the CME core.

HXR emission associated with impulsive electron events

RHESSI clearly established a close correlation of the “interchange reconnection” scenario and the escape of electrons that later form impulsive electron events in interplanetary space (e.g., Krucker et al. 2011). These phenomena correlate in time and magnitude, and also in the spectral hardness of the electron distribution (Krucker et al. 2007). This spectral correlation follows neither the relationship expected for the thin-target or the thick-target model, but lies in

between. More recent analysis by Glesener et al. (2012) of such an event shows the existence of coronal HXR emission, further corroborating the interchange-reconnection scenario.

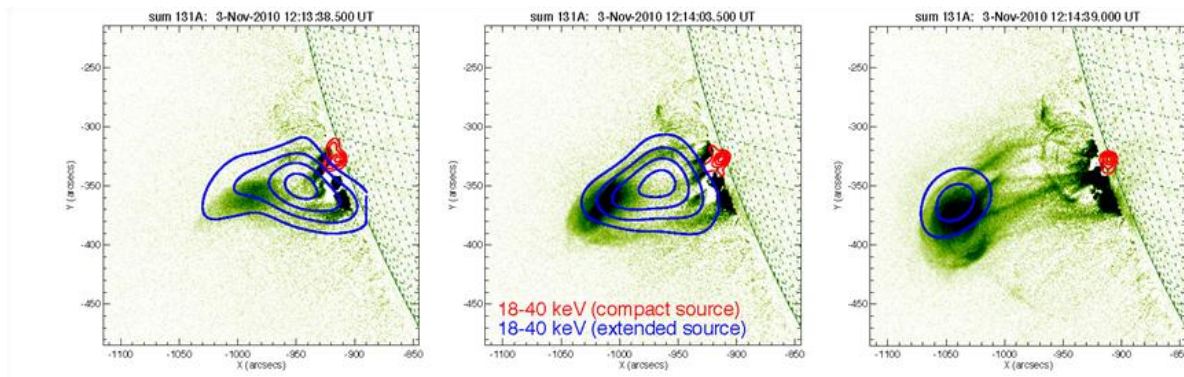


Figure 1-5. RHESSI and SDO/AIA 131Å imaging of an escaping CME. The three frames, taken about 30 s apart, show the escaping CME core in EUV (green image) and HXR (blue contours). The red contours show HXR emission from the top of the partially occulted flare loops.

1.2.2 Science Goal 2 – Flare-accelerated Electrons

Questions critical to understanding flares are: When, where, and how are electrons accelerated, and what happens to them after they are accelerated? How can such a large fraction of the energy released in flares appear as energetic nonthermal electrons? Possible explanations draw both on fundamental theoretical properties of the reconnection process and on the observed properties of electron acceleration in reconnection events observed *in situ* in the solar wind, deep in Earth's magnetotail, and in laboratory plasmas (e.g., Zharkova et al. 2011). RHESSI provides crucial and unique information to address this question through observations of the HXR emission (predominantly electron-ion bremsstrahlung) that the accelerated nonthermal electrons produce when they interact with the ambient medium. RHESSI's X-ray imaging spectroscopy capability allows electron distributions in space, energy, and pitch angle to be determined as functions of time during a flare.

1.2.2.1 Properties of the Coronal Acceleration Region

Krucker et al. (2008b) have described many RHESSI HXR sources that are mostly confined to the coronal regions of the flare. Extended HXR emission is detectable from altitudes of up to a few $\times 10^4$ km, and there is a strong correlation with CMEs. Torre et al. (2012) have used the variation of electron spectrum with position in such extended coronal sources, coupled with the electron continuity equation, to deduce the spatial variation of the accelerated electron flux. In a parallel study, Guo et al. (2013) have used these electron flux maps to deduce the extent of the acceleration region and number of particles in it. With knowledge of the number of electrons accelerated per second above a chosen reference energy (straightforwardly deduced from spatially-integrated hard X-ray spectra), they thus determined the value of the specific acceleration rate (electrons s^{-1} per ambient electron) to be $\sim 10^{-2} \text{ s}^{-1}$, a value that was critically compared with the predictions of electron acceleration models, such as large-scale acceleration by sub-Dreicer fields, impulsive acceleration by super-Dreicer electric fields in reconnecting current sheets, and stochastic acceleration mechanisms involving magnetic concentrations associated with fast-mode magnetohydrodynamic waves.

Petrosian & Chen (2010) obtained the looptop and footpoint energetic electron flux spectra for the 2003 November 3 solar flare (Figure 1-6). Comparing the spectra in the looptop and footpoint regions allows them to constrain parameters in models that invoke electron acceleration by a stochastic process involving plasma turbulence. Chen & Petrosian (2012)

extended this work to determine the acceleration model characteristics directly and non-parametrically from RHESSI data. This was then used to constrain different acceleration model parameters. Assuming acceleration by turbulence, they derived the escape, scattering, acceleration and energy diffusion timescales. The results from a few flares imply either the presence of a wave spectrum steeper than that for Kolmogorov turbulence, or breakdown of the random walk approximation used in determining the escape time.

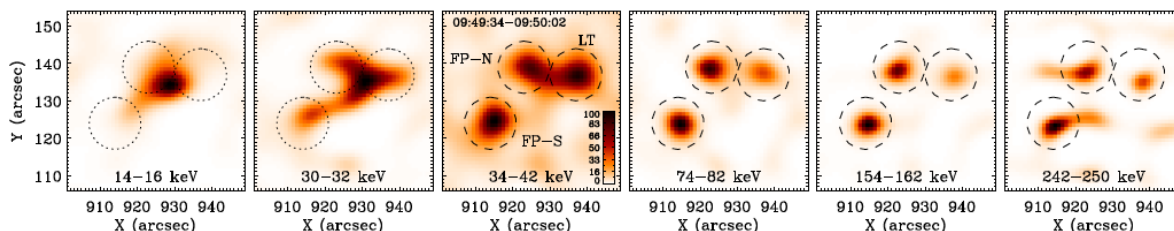


Figure 1-6. Electron flux spectral images up to 250 keV in the 2003 November 03 flare. The images show one loop-top (LT) and two footpoint (FP) sources above 34 keV and a loop structure at lower energies.

1.2.2.2 *Electron Beaming/Directivity*

Hard X-ray sources have an albedo “patch” that results from scattering of primary photons from the dense photosphere. Kontar & Brown (2006) have employed a “dentist’s mirror” approach, which compares the spectra from the primary source and the albedo patch to deduce the directivity of the accelerated electrons. They conclude that the angular distribution of the accelerated electrons is consistent with isotropy. These results suggest (consistent with the known lack of directivity or strong polarization signatures) that the electron beaming must be weak and possibly diffusive. This result, also obtained by Dickson & Kontar (2012), substantially changes our view of the basic thick-target model, inasmuch that the impulsive-phase electrons do not appear to be in free-streaming highly-directional beams.

1.2.2.3 *Use of Coordinated X-ray and Radio Observations*

Radio observations are an ideal complement to RHESSI HXR flare observations since they provide physically distinct perspectives on energetic electrons, hot plasma, and the magnetic field. Combining X-ray and radio observations leads to important new diagnostics:

- Electron spatial, spectral, and temporal distributions can be derived independently from HXR and *microwave* observations. Since the HXRs are density-weighted bremsstrahlung emission, while microwaves are magnetic field-weighted gyrosynchrotron emission from the same population of electrons, coronal magnetic field strengths during flares can be derived at different positions along the flare loop. Estimates of the coronal magnetic field strength and its evolution during a flare are crucial for evaluating flare energy budgets, for understanding particle acceleration, and for investigating the processes involved in CME initiation. Krucker et al. (2010) used radio and hard X-ray observations to derive a magnetic field of ~ 50 G and a nonthermal electron density of a few times 10^9 cm^{-3} within the acceleration region of a flare. These values revealed that during the main energy release, the energy density in the magnetic field is about equal to the energy density of the nonthermal electrons within the acceleration region (i.e. plasma beta is ~ 1 , from a pre-flare value of ~ 0.01) indicating a very efficient conversion of magnetic energy into accelerated electrons in a bulk energization process.
- A major requirement for determining the energy budget in SEEs is information on the low-energy cutoff of accelerated electron distributions (Holman 2012b). Despite the obvious temporal correlation between radio-derived and HXR-derived electron fluxes, there is often a

discrepancy between the spectral indices derived from the two observation sets (e.g., White et al. 2011). Holman (2003) showed that the low-frequency part of the nonthermal gyrosynchrotron spectrum is sensitive to the value of the low-energy cutoff in accelerated flare electrons. This sensitivity has not yet been observationally studied and compared with the electron distribution deduced from X-ray observations.

- Observations of the **sub-millimeter wave** emissions of solar flares above 200 GHz (Kaufmann et al. 2004, Luethi et al. 2004) have revealed a second component with intensities well above an extrapolation of the synchrotron spectrum seen at lower frequencies. Surprisingly, the measurements at two frequencies suggest that the spectrum of this new component increases with increasing frequency in contrast to the microwave synchrotron spectrum. This exciting new finding has prompted many suggested explanations (e.g., Fleishman & Kontar 2010, Krucker et al. 2013) but the emission mechanism(s) of this new component remain(s) unidentified.
- Low-frequency **decimeter-wave** and **meter-wave** emission comes generally from higher in the corona and shows coherent emission from energetic electrons associated with escaping electron beams, plasmoid ejecta, and CMEs (e.g., Battaglia & Benz 2009). RHESSI also observes the high corona (e.g., Krucker et al. 2008b) and brings a similar quantitative complement as described above for the microwave frequencies. The extended VLA provides for the first time imaging spectroscopy above 500 MHz, i.e. above the Nançay Radio Heliograph frequency range. First results of combined RHESSI and EVLA observations reveal the trajectory of escaping electron beams relative to the flare site seen by RHESSI (Chen et al. 2013).

1.2.3 Science Goal 3 – Flare-accelerated Ions

Measurements of nuclear de-excitation lines, the positron-annihilation line at 511 keV, and the neutron-capture line at 2.223 MeV in flares can reveal not only the composition, spectrum, and angular distribution of the accelerated ions, but also the density and composition of the solar atmosphere in which the ions interact. RHESSI provides measurements of all of these gamma-ray spectral features for the largest and most energetic solar flares, and it has observed the neutron-capture line in tens of flares. The results obtained have been both remarkable and unexpected, providing evidence for non-vertical guiding magnetic fields (Smith et al. 2003), an as-yet unexplained broadening of the narrow solar annihilation line (Share et al. 2003, 2004), and clear evidence of accelerated ions and electrons interacting at different locations (Hurford et al. 2003, 2006). In past solar cycles, the declining phase has often been the time when such large events tend to occur. Detection of just a few more of these events will advance these studies considerably, particularly with the far-superior complementary observations from other observatories that are now available.

1.2.3.1 *Location and Extent of Gamma-ray Source(s)*

RHESSI has produced the only high-resolution imaging of flare gamma rays (Hurford et al. 2003, 2004), with an angular resolution of 35 arcseconds. The gamma-ray sources of the 2.223 MeV neutron capture line showing where ions stop in the atmosphere were found to be separated by up to tens of Mm from the bremsstrahlung HXR sources that reveal where accelerated electrons stop. This result strongly suggests distinct acceleration processes for the ions and electrons. Flares that produce sufficient gamma-ray emission for such imaging studies are rare, and so there is an urgent need is to continue observing through Cycle 24 to extend and further develop these remarkable results.

1.2.3.2 Energy, Spectrum and Composition of Energetic Ions, and Composition of Target Plasma

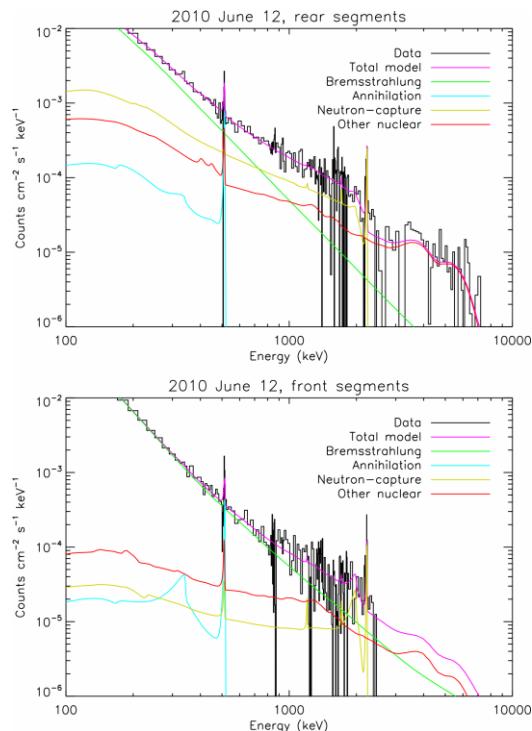


Figure 1-7. Fit to the 2010 June 12 gamma-ray spectrum showing the best fit components using the rear (top) and front (bottom) segments separately. The front segments do not extend as high in energy, and the neutron-capture line is a ~ 4 -sigma detection, compared to a ~ 5 -sigma detection in the rear segments.

The RHESSI gamma-ray count-rate spectrum for the first gamma-ray flare of Cycle 24 (on 2010 June 12) is shown in Figure 1-7. This M2 flare shows the various signatures of energetic ions on top of a bremsstrahlung continuum from relativistic electrons: the positron-annihilation line and continuum, the neutron-capture line at 2.223 MeV, and a combined nuclear-emission template for narrow de-excitation lines (from accelerated protons/alphas on ambient heavy nuclei), broad de-excitation lines (from accelerated heavy nuclei on ambient H/He), and α - α fusion lines. These nuclear-emission templates were calculated for certain abundances assumptions, the heliocentric angle of the flare, and various values of the α/p ratio and proton spectral index based on the significantly improved gamma-ray line production code of Murphy et al. (2009).

In strong flares where there is sufficient flux to resolve the narrow lines, these nuclear-emission templates can be compared with the data to determine the best-fit ambient composition, accelerated composition, spectral index for accelerated ions, and α/p ratio. In even stronger flares, multiple intervals of the flare can be separately fit to investigate changes over the course of the flare (Shih et al. 2011). In two flares, RHESSI observations indicate that both the ambient and accelerated compositions are consistent with coronal abundances. The best-fit power-law spectral indices for accelerated protons between 5 and 30 MeV are in the range of 4–5, and appear to soften over the course of these flares.

and appear to soften over the course of these flares.

Even though RHESSI can measure energy losses in the germanium detectors only up to 17 MeV, higher-energy photons, mostly from pion-associated emission, will produce a predictable continuum of counts in the RHESSI energy range. In 2009, a new round of Monte Carlo simulations was undertaken to produce a fuller model of RHESSI's instrument response to such higher-energy photons. The range of the simulations was extended from the original limit of 20 MeV to 150 MeV to accommodate modeling the response of the instrument to pion-produced gamma rays. This pion-decay contribution is visible in the most energetic flares, such as 2005 January 20, and enables estimates of the accelerated proton spectra to be extended to at least 300 MeV.

1.2.3.3 Correlated Electron and Ion Acceleration

RHESSI observations have shown that the rate of acceleration of >30 MeV protons is closely proportional to the rate of acceleration of relativistic (>300 keV) electrons, while the acceleration of non-relativistic electrons (that presumably heat the SXR-emitting plasma) is only

proportional when the proton acceleration exceeds a threshold (Shih et al. 2009). Figure 1-8 shows the RHESSI measurements from 2002 to 2005 (29 flare events) of the 2.223 MeV neutron-capture gamma-ray line and >300 keV electron bremsstrahlung continuum emissions.

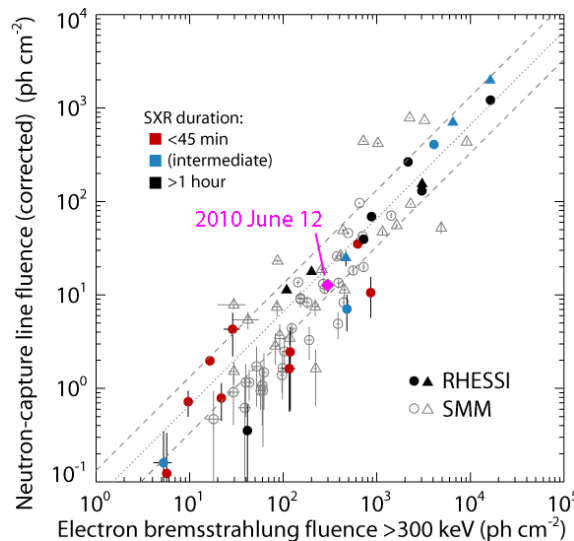


Figure 1-8. Correlation plot between neutron-capture line fluence (corrected for limb darkening) and >300 keV bremsstrahlung fluence for flares with heliocentric angles <80°. Circles (triangles) represent flares with complete (incomplete) coverage. The magenta diamond near the center of the plot is the 2010 June 12 flare from this solar cycle, while the other solid points are from Cycle 23, hollow points are from Cycles 21 and 22.

These two energies are tightly correlated over more than three orders of magnitude in fluence, from the largest flares down to the limits of detectability. All flares fall within a factor of two of the best-fit line, except for four flares with marginal (~1–2 sigma) line detections. Furthermore, all RHESSI events with >300 keV bremsstrahlung are consistent with having a neutron-capture line. These observations are consistent with two (possibly concurrent) acceleration processes: one that accelerates both >30 MeV protons and >300 keV electrons in roughly proportional amounts, and another that accelerates electrons above 50 keV but not above 300 keV.

Figure 1-8 also includes a point (the magenta diamond near the center of the plot) for the RHESSI observation of the 2010 June 12 flare, and thus includes events from four solar cycles. The correlation observed by RHESSI for Cycle 23 appears to be stronger than that observed by SMM for Cycles 21 and 22. Thus, it is important to observe additional events through Cycle 24 to see how the correlation evolves.

1.2.3.4 Phases of Particle Acceleration

RHESSI's breadth in hard X-ray and gamma-ray imaging spectroscopy has added considerable clarity to understanding the variety of acceleration mechanisms at work during flare/CME development. The bifurcation of SEP morphology into "shock" and "flare" populations (e.g., Reames 2013) is clear, but within the flare itself we can now distinguish several apparently distinct processes, in which the signatures come from the low corona/chromosphere; in some cases shock-related physics may play a role even in this domain.

The 2005 January 20 flare was accompanied by a Ground Level Event (GLE) where protons with energies in excess of 5 GeV were observed at Earth within 6 minutes of the onset of the impulsive phase of the flare. RHESSI's spectroscopic measurements have revealed two distinct phases of particle acceleration during the few minutes of the flare. The nuclear de-excitation time profile was fit using a loop model and the >300 keV HXR profile as a proxy for the ion acceleration profile before 06:45:40 UT, with an extrapolation to later times. A similar analysis was carried out for the 2.223 MeV line flux, taking into account the ~100 s delay in this line due to the slowing down time of the neutrons.

A second particle-acceleration phase commencing at ~06:45:40 UT is suggested by the striking increase in both >20 MeV and 2.223 MeV photons (Masson et al. 2009) – six times as many protons >30 MeV were accelerated in the second phase compared to the first. The rise time of the second acceleration phase appears similar to that observed in the neutron monitor rates observed at the South Pole, suggesting this second phase is associated with the injection

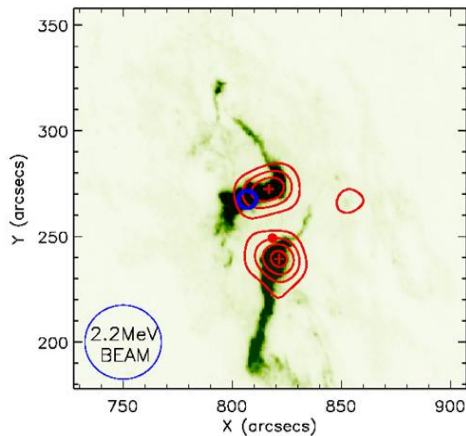


Figure 1-9. RHESSI image of the 2005 January 20 flare. Red contours: >300 keV HXR sources; small blue circle: centroid of 2.2 MeV source.

of high-energy particles into space. It is possible that both RHESSI and Fermi will jointly detect another such event having distinct acceleration phases.

RHESSI has imaged both hard X-rays and the neutron-capture line (Hurford et al. 2006) between 06:44 and 06:56 UT (Figure 1-9) showing that the hard X-rays primarily come from two footpoints, but the 2.223 MeV line photons appear to come from a region centered near the northern footpoint. Since most of the 2.223 MeV line photons were produced during the second acceleration phase, it is interesting to speculate that the protons in this second phase came from the same acceleration process that produced protons in the GLE - only a fraction of them were able to reach the solar surface via open field lines that happened to be close to the northern footpoint.

1.2.4 Science Goal 4 – Flare-heated Plasma

This goal addresses plasma at all flare temperatures. RHESSI is sensitive to the hottest plasmas with temperatures above ~8 MK. This complements many other instruments operating at longer wavelengths, both in space and at ground-based observatories, which are sensitive to thermal plasma over a wide temperature range below the highest temperatures deduced from RHESSI spectra (~30 – 50 MK). The differential emission measure can thus be determined with unprecedented reliability (e.g., Hannah & Kontar 2012, Caspi et al. 2013). RHESSI is also sensitive to the accelerated electrons that are thought to be most likely responsible for the heating of this plasma in the impulsive phase of flares.

1.2.4.1 *The Flaring Lower Solar Atmosphere*

This topic includes flare ribbons and footpoints, white-light flares, and the excitation of sunquakes.

SORCE observations of total solar irradiance have confirmed the importance of the lower solar atmosphere during the impulsive phase of flares in the overall energetics of SEEs (Woods et al. 2004; Kretzschmar 2011). The data confirm that the white-light (WL) flare continuum and its extension into the UV dominate the radiated energy. The possible mechanisms for this continuum emission – blackbody radiation, hydrogen recombination, and H⁻ emission via “back-warming” – are still being discussed inconclusively. Recent radiative hydrodynamic simulations (Allred 2005) favor Balmer continuum and H⁻ emission as sources of enhanced WL emission, while Kretzschmar (2011) has found that SoHO/VIRGO observations of WLFs match blackbody radiation at a temperature of 8,500 K, consistent with what is found for many stellar flares (e.g., Kowalski et al. 2012). As a result, many modern instruments are now beginning to focus on diagnosing the response of the chromosphere, particularly during a flare’s impulsive phase (SOT and EIS on Hinode, AIA and EVE on SDO, the soon-to-be-launched IRIS mission, as well as several ground-based instruments such as ROSA, IBIS, FISS, etc.).

While these instruments typically diagnose the chromospheric response through optical, UV or EUV observations, RHESSI remains the only instrument capable, through a unique combination of HXR imaging and spectroscopy, of determining the location of the energy deposition and the properties of the nonthermal electrons deemed to be responsible for driving

these emissions. The flare radiation is driven by intense energy deposition into the footpoints of coronal magnetic structures, and hard X-ray bremsstrahlung from nonthermal electrons reveals these footpoints. RHESSI imaging spectroscopy of the nonthermal hard X-ray emission thus provides essential and unique information on the location and energetics of the process. The hard X-ray footpoint sources are more localized than the UV-H α ribbons, but are so intense that they may be unresolved both spatially and temporally with the best available instruments. The HXR observations provide the most precise diagnosis of the impulsive-phase energy release.

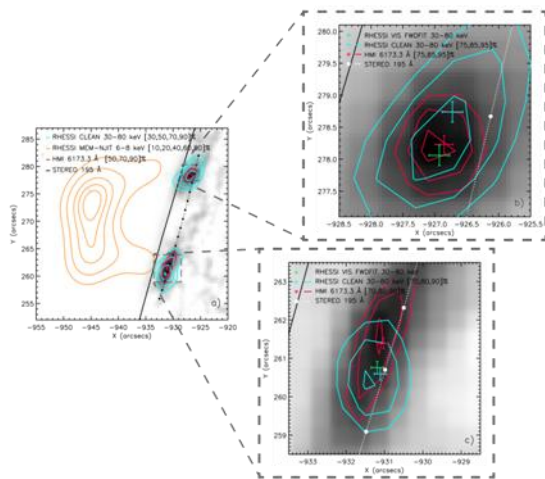


Figure 1-10. Observations by RHESSI (30-80 keV HXR: blue contours) and HMI (white-light continuum: red contours) of a flare on 2011 February 24. This flare was also observed by STEREO-B at almost its apparent disk center, and the black/white chain line shows the projected height of the solar photosphere as seen from the Earth-perspective observations.

Figure 1-10 shows an example of how RHESSI and other instruments (HMI and STEREO-B, in this case) work together at the highest angular resolution, with coalignment at the sub-arcsecond level (Martinez Oliveros et al. 2012). These observations have enabled the first direct determination of the actual physical height of a white-light flare. The WL and HXR emissions coincide at both footpoints consistent with the source being at the lowest possible altitude, i.e., that corresponding to $\tau = 1$.

Generally a white-light flare is one that is powerful enough to perturb the actual photosphere of the Sun; as discovered by Carrington over 150 years ago, such an event may double the solar luminosity over its area. Now we have many examples of the even deeper phenomenon of the flare acoustic wave (sunquake) propagating in the interior of the Sun. *Neither the white-light flare nor the sunquake have consensus explanations yet.* Each is closely related to the energy of the accelerated electrons as revealed by the HXR observations.

1.2.4.2 Chromospheric “Evaporation”

RHESSI observations provide critical information about both the energy distribution of accelerated electrons and the flare plasma with which they interact. The comparison of these X-ray observations and the data now available at longer wavelengths with contemporary flare models enables a previously unattainable understanding of the heating and evolution of flare plasma.

The variation of X-ray centroid location with energy in specific events allows the density structure in the chromospheric footpoints of the loops to be determined. Using a collisional energy-loss model, Prato et al. (2009) find a density profile that is not consistent with that in the quiescent (or even active region) chromosphere, but is consistent with the density profile expected in the dynamic environment of an atmosphere heated by a flare-accelerated electron beam. Saint-Hilaire et al. (2010) have applied this type of analysis to a set of 838 flares observed in HXR above 25 keV to determine, in a statistical manner, the chromospheric and coronal density profile of the flaring solar atmosphere. Their “average flaring atmosphere” was found to have a density scale height of (0.13 ± 0.02) Mm at low altitudes and (5–6) Mm at coronal altitudes, with a height of (1.3 ± 0.2) Mm for the transition between these regions.

The evolution of the X-ray spectrum in specific events showing a mild spectral break can be used to deduce the column density of fully ionized plasma and its evolution during the impulsive phase of the flare. Su et al. (2011) found the column density to increase by a factor of 350 in

one flare. Since the spectral break was found to result from the plasma ionization structure, the accelerated electron spectrum was found to be a single rather than a double power law in electron energy.

The physics of the lower solar atmosphere during the impulsive phase of a flare, during which pressure gradients produced by spatially-varying flare heating drives upward mass motions in a process termed (somewhat erroneously) chromospheric “evaporation,” is now the focus of several lines of numerical modeling. These include basic plasma physics (e.g., to describe magnetic reconnection or particle acceleration), MHD in 3D and possibly a two-fluid approach in the future, and 1D radiation hydrodynamics analysis of individual flare loops (e.g., Allred et al. 2005). The radiation-hydrodynamic simulations use detailed optically-thick non-LTE radiative transfer, thus including radiation produced throughout the solar atmosphere as a heating and cooling mechanism. The output radiation predicted by these models can then be compared directly with chromospheric and coronal observations taken with the instruments mentioned above, thereby furthering our understanding of the processes at work in the complex layers of the Sun’s atmosphere. For consistency, it is critically important to use the electron beam parameters determined from RHESSI observations as inputs to these simulations.

This technique has been applied using RHESSI and EVE observations of the flare shown in Figure 1-11. The accelerated electron flux spectrum was derived from the RHESSI spatially-integrated nonthermal HXR spectra with a footpoint area of 10^{17} cm^2 , estimated from RHESSI images. The model-predicted fluxes in several EUV lines and continua (dashed lines) can be compared with the EVE measured fluxes (solid lines, from Milligan et al. 2012) to reveal detailed physics of the particle and radiative interactions within in the flaring chromosphere and the depth at which the electrons lose their energy. This will help with the long-standing white-light flare problem. Any discrepancies between model predictions and observations could be attributed to, for example, an overestimation of the low-energy cutoff or footpoint area, which will help to refine the analysis. These models are currently being adapted to include co-spatial proton beams and electron return currents.

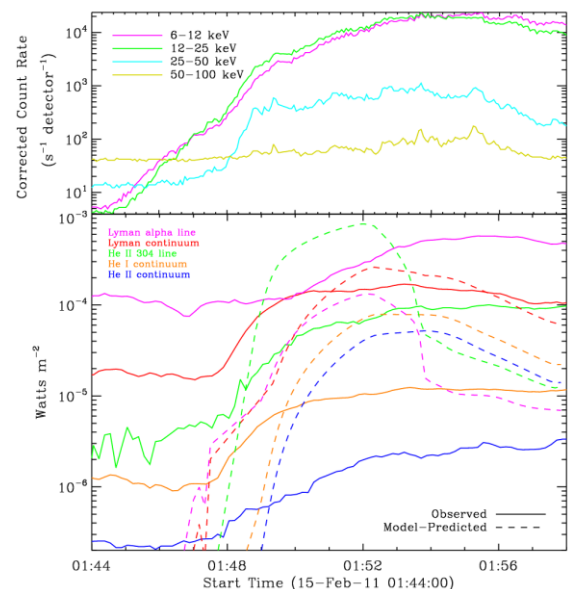


Figure 1-11. Top: RHESSI X-ray light curves for a flare on 2011 February 15. Bottom: Light curves for several line and continuum transitions, both observed with EVE and calculated using the Allred et al. (2005) model driven by the electron beam distribution derived from RHESSI HXR spectra.

1.2.4.3 Microflares, Nanoflares, and the Solar Cycle

Small solar flare-like events occur much more frequently than flares, and the analysis of the distribution function of their associated energies has become a major topic of research. An associated question is whether these small events are similar to their larger cousins. RHESSI has contributed greatly to this subject, owing to its sensitivity, low-energy response, and capability for imaging spectroscopy of these weak events.

The RHESSI real-time generation of flare magnitudes and locations into a quick-look catalog has made several statistical analyses readily possible. The precise position determinations from RHESSI imaging have many potential applications to statistical studies of flare occurrence. Christe et al. (2011) used the systematic deviations of source positions across the disk to study

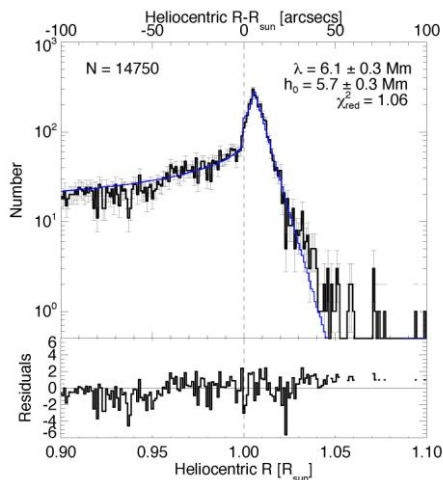


Figure 1-12. Limb distribution of 14,750 RHESSI flares, showing the expected limb brightening in the outermost 10% of the disk, plus the concentration above the limb resulting from finite source heights. The lower panel shows residuals against a simple model for the height distribution.

flare height structures via their projected positions shown in Figure 1-12. This initial study determined the height distribution of these thermal events as best fit with an exponential distribution with a scale height of (6.1 ± 0.3) Mm above the photosphere. This suggests that microflares generally occur lower down in the solar corona compared to large flares, though, as found in Hannah et al. (2010), they are not necessarily smaller.

Baylor et al. (2011) used more than 4,500 RHESSI microflares to investigate the electron densities and volumetric filling factors using cooling time analysis. They found that the necessary filling factors to match the observed cooling times is very small, a mean of order 10^{-4} . Such a small value suggests that the physical assumption that no heating occurs after the main phase is not correct. Multi-wavelength studies of microflares show flows and thermal responses that are similar to large flares (Berkebile-Stoiser et al. 2009, Brosius & Holman 2010).

The nanoflare hypothesis remains a viable explanation of the apparently continuous heating of coronal plasma (e.g., Klimchuk 2006). Whereas RHESSI does not detect individual nanoflares in the non-active-region corona, it has been able to detect a

general level of HXR emission from the quiet Sun (e.g., Hannah et al. 2010).

The patterns of flare occurrence in general lead to knowledge of how the solar magnetic cycle develops, and we are beginning to see applications of the RHESSI database in this area (Hudson 2007; Schrijver et al. 2012). Note that the RHESSI active lifetime now spans the “extended minimum” between Cycles 23 and 24, and in principle may be able to extend through most of Cycle 24.

1.2.5 Science Goal 5 – Global Structure of the Photosphere

Because of its requirement for sub-arcsecond aspect information, RHESSI incorporates correspondingly precise tools for image alignment, including the solar aspect system (SAS, described in Section 2.2.3). These requirements resulted in a major significant additional capability for RHESSI to study the Sun at visible wavelengths with a rapidly rotating telescope in space, a method never previously employed. The SAS consists of three 4-cm diameter simple lenses that focus solar images in the continuum at 670 nm onto three linear CCDs 1.5 m away. The measured limb profiles (six in all, typically at a rate of 16 sets s^{-1}) provide the instantaneous pointing direction of the RHESSI instrument with sub-arcsecond accuracy. The rapid rotation of RHESSI ($\sim 15 \text{ rpm}$) around the solar direction provides another major advantage, since it greatly simplifies flat-field corrections, temperature corrections, and other factors that make photometry difficult at the parts-per-million level.

Fivian et al. (2008) have used these capabilities to obtain the most precise measure of the solar oblateness, defined as the excess of the equatorial radius over the polar radius. Using only three months of the available data at an intermediate state of solar activity and screening against contamination by magnetic features at the limb, they reported a solar oblateness value of (8.01 ± 0.14) milli-arcseconds. This is consistent with the Dicke estimate of 7.98 milli-arcseconds expected from the rotation of the Sun taken as a solid body. It exceeds in precision all other measurements (both space and ground), including the recent one from SDO

(Kuhn et al. 2012). Further work with these data will define the pole-to-equator temperature gradient, the facular limb-darkening coefficient, and related observational problems of classical solar astronomy.

1.2.6 Science Goal 6 – Nonsolar Objectives

1.2.6.1 *Terrestrial Gamma-Ray Flashes (TGFs)*

TGFs, millisecond pulses of gamma radiation from lightning, have become a very active field of research worldwide, thanks in large part to RHESSI observations over the past decade. RHESSI was the second spacecraft, after the Compton Gamma-Ray Observatory, to record TGFs. However, many more were detected than expected (well over 1,000 to date), and the energy spectrum was unexpectedly found to extend up to >20 MeV.

TGFs are momentarily as intense as an X-class flare seen in RHESSI's detectors, despite the terrestrial source being over 600 km away. They may pose a radiation health risk to airline passengers (Dwyer et al. 2010), and evaluating this possibility is a primary motivation for future work with RHESSI. Although it is now known, thanks to RHESSI data, that TGFs are associated with intra-cloud lightning, it is still not known whether they trigger these flashes or are a side-effect of them; it is also not known if TGFs ever proceed without lightning, and if they accompany other storm phenomena such as blue jets and sprites. The underlying radiation mechanism of a TGF is bremsstrahlung from relativistic electrons produced by "relativistic runaway avalanche," a process of interest to high-energy solar physicists and astrophysicists as well, since it is related to sub-Dreicer acceleration in plasmas. How and where in the thundercloud this avalanche takes place are further unanswered questions that future RHESSI observations can address.

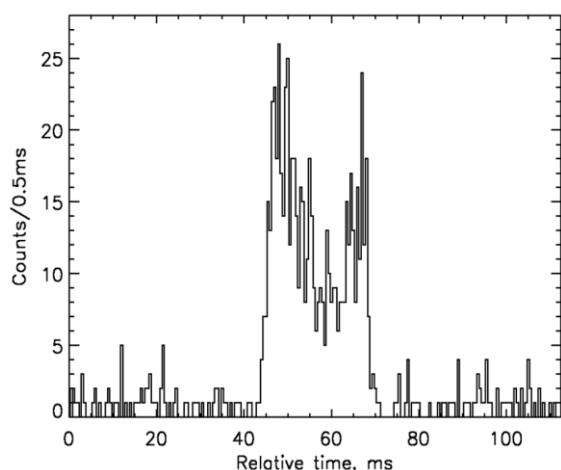


Figure 1-13. TGF particle beam event of 2013 Jan 18. RHESSI rear-segment count rates above 30 keV.

On January 18, 2013, RHESSI saw its most intense TGF (Figure 1-13), but in this case the detector counts were produced by charged particles rather than by gamma-rays. The unique time profile, much longer than the typical <1ms TGF, has all the characteristics expected for the current TGF model in which an electron/positron beam is produced above a lightning storm via Compton scattering and pair production by the TGF gamma-rays in the upper atmosphere. This beam of particles travels along the magnetic field line that happened to pass through the RHESSI spacecraft to produce the first count-rate peak. The second peak some 20 ms later is produced after the particles are mirrored at high geomagnetic latitude and pass back through the instrument along the same field line. A 511 keV positron annihilation line is clearly visible in the

RHESSI energy spectrum confirming the presence of positrons in the beam.

1.2.6.2 *Cosmic Gamma-Ray Bursts (GRBs)*

Thanks to its broad energy range and wide field of view ($>2\pi$ sr), RHESSI has made valuable contributions to the study of cosmic gamma-ray bursts (GRBs). These energetic transients have peak energies ranging from tens to hundreds of keV, and RHESSI continues to be a useful tool for continuum spectroscopy of GRBs (Bellm 2010; Ripa et al. 2012). RHESSI is also assisting with the prompt localization of GRBs (123 to date, K. Hurley, private

communication) as part of the Interplanetary Network (IPN), which localizes GRBs by triangulation, comparing the time profiles seen by spacecraft in different parts of the solar system. Prompt localization permits rapid follow-up by telescopes at all wavelengths from radio to X-rays, providing data on both the source of the explosion and the environment in the host galaxy.

1.3 How the Prioritized Science Goals will be achieved

The next three or four years of enhanced solar activity provide us with a golden opportunity to exploit the full potential of the HSO. RHESSI will be a key player, providing unique information on the hottest plasma and the energetically important electrons and ions. The primary requirement for achieving the PSGs is for RHESSI to continue to provide X-ray and gamma-ray imaging spectroscopy during the declining phase of the current solar cycle. **No other instrument can provide the location and spectra of the highest temperature plasma and of the flare-accelerated electrons and ions, information that is crucial for achieving all of these goals.**

In addition to the existing HSO space assets, eagerly anticipated new radio capabilities are expected to be available during this same time period, providing invaluable imaging spectroscopy observations over wide frequency ranges. These include several new major facilities, such as the Expanded Very Large Array (EVLA) and ALMA (mm-wave), but **the main new strength lies in the Expanded Owens Valley Solar Array (EOVSA). We have never before had simultaneous microwave and RHESSI hard X-ray imaging spectroscopy, and this is the key to many problems of flare and active region development.** The two spectral bands show aspects of the same phenomena with distinctly different physical processes. In the past, we have had hints of this capability from the fixed-frequency “slices” of the microwave spectrum, and with EOVSA we will now get the full and detailed spectrum of the radio emission at every point in the image, and at every moment in time. EOVSA comes on line this year (2013), and we expect that the first few M-class events will produce breakthrough observations – for which the RHESSI hard X-rays are required to establish “ground truth.”

Finally, we note a comparable qualitative breakthrough in ground-based observations of the lower atmosphere, leading up to ATST. Several observatories (e.g., the Dunn Solar Telescope) now have broad-band capability for imaging spectroscopy in the energetically crucial photosphere and chromosphere. Likewise, IRIS (to be launched in 2013) promises SUMER-like observations of flares for the first time, and again RHESSI hard X-rays are required to establish “ground truth” for the energetics.

1.3.1 Science Goal 1 – Evolution of Solar Eruptive Events

With the subsequent increased level of solar activity that is expected to peak in 2013, future work will focus on synthesis of RHESSI observations with SDO/AIA and a host of other observations. Such a comprehensive data set will allow us, for example, to test the ubiquity of the magnetic evolution scenario discussed in Section 1.2.1.1 and the breakout reconnection picture discussed in Section 1.2.1.2. The SDO/AIA instrument provides us with unique possibilities to obtain detailed insight into the earliest phase of CME initiation and its plasma environment (Section 1.2.1.4) through its high-cadence imaging over a broad range of temperatures. Combined with RHESSI’s observations of the particle acceleration in the associated flares and SDO/HMI observations of the magnetic field configuration and changes, these studies will provide us with detailed insight into the initiation of the instabilities and magnetic reconnection driving eruptive events.

The occurrence of solar energetic particle events has a strong solar-cycle dependence, and we expect many outstanding events to occur in the next years. To the pioneering work on the relation between flares, CMEs and SEPs (Section 1.2.1.5), we can now add information from

SDO, Fermi, and several new ground-based facilities for radio astronomy. The two STEREO spacecraft, together with WIND and ACE, will provide *in situ* measurements of SEPs at widely separated solar longitudes. Additionally, SDO/AIA will provide the high time cadence observations that were missing for observations taken during the last solar maximum. By tracking the electrons, imaged at the Sun using RHESSI HXR imaging spectroscopy data, through the interplanetary medium using the Type III radio emission, to the *in situ* detection by the Wind and STEREO spacecraft, we can trace and study the magnetic connectivity from the Sun to the Earth.

The energy partition study of Emslie et al. (2012; Section 1.2.1.3) was restricted to 38 large SEEs, for which the dynamic range was comparable to the order-of-magnitude observational scatter, so that no clear variation in the partition of energy with flare size could be determined. A greater range of event sizes is needed to study the variation of these ratios, and thus to determine how the partitioning of the released energy does (or does not) vary with the overall energy in the event. Such an objective analysis requires that we exclude, to the maximum extent possible, any selection effects in identifying “events.” To this end, we will conduct the temporal equivalent of an astronomical “deep-field” approach, in which all the events from a given time interval (e.g., the passage of an active region across the solar disk) are studied. Such a study will involve all of the instruments in the HSO, with RHESSI playing its usual pivotal role in assessing the energies in flare-accelerated particles.

1.3.2 Science Goal 2 – Flare-accelerated Electrons

We expect a dramatic increase in our understanding of coronal HXR sources (Section 1.2.2.1) by combining RHESSI observations with those from Hinode, STEREO, and SDO. RHESSI can identify the coronal regions, both pre-flare and during the impulsive phase, that appear to be the sites of flare energy release, magnetic reconnection, and electron (and ion) acceleration. EOVSa will provide essential complementary observations of the accelerated electron populations, and will give us quantitative measurements of the magnetic field strength within the coronal acceleration region. Hinode/XRT provides imaging of these high-temperature regions. Comprehensive differential emission measure analysis is being carried out using the newly available multiwavelength line intensities from AIA and EVE but RHESSI data are critical for this effort too in anchoring the distribution at the highest temperatures. EIS imaging spectroscopy provides the key measurements of flows and turbulence in these regions to clarify the energy release and particle acceleration processes (Section 1.2.2.2). STEREO/EUVI provides 3-D observations of flare loops seen in EUV, SDO/AI provides high cadence imaging of the whole Sun in multiple wavelengths, and SDO/EVE provides spatially integrated UV/EUV spectroscopy over a wide wavelength range. SDO and Hinode vector magnetograms are the first from space, and their high resolution allows the development of more accurate coronal field models and the tracing of the field evolution during a flare for comparison with reconnection models.

Krucker et al. (2007, 2008a) found evidence that essentially all CME events can be observed in hard X-rays as extended, and often moving, sources in the high corona. The new complementary information provided by SDO, Fermi, and NuSTAR, and new radio facilities such as EOVSa and EVLA, will allow us to follow up on these discoveries with more explicit identification with specific acceleration mechanisms (Section 1.2.2.3). These new radio telescopes will allow us, for the first time, to systematically image the different types of coherent radio bursts that identify the different locations of electron acceleration in the lower corona within solar eruptive events.

RHESSI’s limited imaging dynamic range frequently restricts the ability to study relatively weak coronal HXR sources in the presence of the much brighter footpoints. However, about 10% of all flares are usefully occulted so that the footpoints are obscured from view. In those

cases, RHESSI can study the coronal source(s) in isolation. In the past, the magnetic configuration of such near-limb events could not be determined, but now STEREO can provide information about the magnetic structure when the flare is not occulted as seen from at least one of the two spacecraft. In addition, EUV ribbons imaged with STEREO show the likely location of the occulted HXR footpoints, and the CME geometry seen with the STEREO coronagraphs can be compared with the HXR coronal source location(s).

1.3.3 Science Goal 3 – Flare-accelerated Ions

RHESSI gamma-ray observations during the declining phase of Cycle 24 are dependent on the operational state of the spectrometer (discussed in Section 2.2.1) and the level of solar activity. Radiation damage has broadened the spectral resolution of the rear detector segments and reduced their effective sensitive volume, an effect mitigated by periodic anneals. For about a year after each anneal, the rear segments are still able to achieve spectral resolutions of less than a few tens of keV in the MeV range, still significantly better than the Fermi GBM BGO detectors. For two or three years after an anneal, before the level of radiation damage becomes severe, the FWHM spectral resolution of the front segments is a few keV up to a maximum energy of >2.3 MeV, so that it is possible to use the front segments to detect and study intrinsically narrow lines such as the annihilation and the neutron capture lines. In comparison to the rear segments, the front segments have smaller photo-peak efficiencies ($\sim 50\%$ at 511 keV and $\sim 15\%$ at 2.2 MeV) and greater deadtime at the most intense peaks of flares, but they also have lower background, so comparable science up to 2.3 MeV can still be achieved (see Figure 1-7 for a comparison). Even with unsegmented detectors, RHESSI will be sensitive to gamma-rays and to the neutron-capture line in large flares but with degraded energy resolution.

With accurate simulations of gamma-ray spectra from accelerated protons and heavier ions over a wide range of energies, an alternative method for performing RHESSI spectral analysis (Section 1.2.3.2) is being developed in which the standard forward-fit parametric (e.g., power-law) approach is replaced by the application of regularized inversion techniques. These techniques require no *a priori* knowledge of the form of the proton/ion spectra, and have proved effective in the identification of features in electron spectra from analysis of HXR spectra (e.g., Piana et al. 2003). As pointed out by Emslie et al. (2012), a nonparametric determination of these spectra will enable a more accurate determination to be made of the total energy content in accelerated protons and ions.

Visibility-based analysis techniques will improve the quantitative comparison of the locations of electron and ion impact zones through imaging of the 511 keV and 2.223 MeV line sources in large gamma-ray flares (Sections 1.2.3.1 and 1.2.3.3). Since the 511 keV line is more effectively attenuated by thinner (and thus finer) grids, RHESSI can image 511 keV photons with much finer angular resolution (~ 10 arcsec vs. 33 arcsec) than for the 2.223 MeV neutron-capture line, but visibilities are needed to remove the contamination by the underlying bremsstrahlung continuum. RHESSI imaging studies of these lines can be compared with centroid locations as accurate as ~ 30 arcsec found by Fermi/LAT at energies above ~ 500 MeV in sustained gamma-ray events in the hours following M- and X-class flares (e.g., Omodei et al. 2012 and Section 1.2.3.4). These events fall into a category defined by Ryan (2000) as long-duration gamma ray flares (LDGRF), and their origins have yet to be determined.

We will also continue our analysis of joint RHESSI/Fermi observations. We are currently preparing a catalog of Fermi LAT observations of sustained γ -ray events based in part on RHESSI detections of hard X-rays above 100 keV and CMEs with speeds >750 km s $^{-1}$. RHESSI covers the same energy range as GBM but with significantly improved spectral resolution. The LAT extends the range up to several hundred GeV. RHESSI can observe the low-energy portion of the pion-decay spectrum detected >100 MeV by LAT. However, before we can obtain accurate determinations of the spectrum of >300 MeV protons responsible for the

associated component of the gamma-ray emission observed by RHESSI, an important improvement is required in the pion-decay spectral code to take into account scattering of photons deep in the solar atmosphere.

A Fermi GI program (B. R. Dennis, PI) is providing ready on-line access for the solar

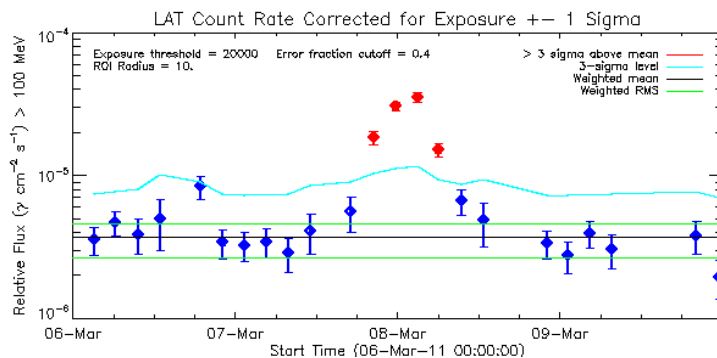


Figure 1-14. LAT flux for a four-day period showing the increase in red from the flare starting on 2011 March 7.

scientific community to both GBM and LAT flare observations. It allows joint spectral and time-series analysis to be carried out using well-tested RHESSI software. Quick-look light curves of both GBM and LAT solar data are also available on the RHESSI Browser discussed in Section 1.4.3. The example of a four-day LAT light curve shown in Figure 1-14 reveals the first sustained emission event detected with LAT following an M-class flare on 2011

March 7. RHESSI has set limits on the 2.223 MeV neutron capture line during this flare and during the times of delayed high-energy emission allowing limits to be set on the accelerated proton spectra below 300 MeV during these time periods.

1.3.4 Science Goal 4 – Flare-heated Plasma

With space-based data from Hinode, SDO, and IRIS, plus data from several new ground-based radio and optical observatories leading up to and including ATST, we will be able to make coordinated multiwavelength imaging-spectroscopy observations that also include RHESSI X-ray data. In addition to the powerful diagnostic value in studying the response of the upper atmosphere and chromosphere to flare heating (Section 1.2.4.2), there is every hope that this can be done for white-light flares (Section 1.2.4.1) and sunquakes.

Microflare observations by RHESSI and, for example SDO, will provide complementary information about the distribution of temperatures of the heated plasma allowing for a better estimate of the thermal energy (Section 1.2.4.3). Several studies are already underway (Inglis et al. 2012, Hannah & Kontar 2012). Microflare observations will also be extended into the domain of solar-cycle variations. Flare activity reflects the most extreme form of magnetic stress of the solar atmosphere, and its patterns of behavior must reflect the sub-photospheric sources of the stress. For this purpose, the longer the time series of the data, the better. Specifically we can hope to detect and characterize spatio-temporal correlations that will guide us to the interior origins of the highly stressed fields. This kind of information will complement other empirical approaches (e.g., helioseismology) to the characterization of the solar dynamo and the interior magnetic structure of the convection zone.

1.3.5 Science Goal 5 – Global Structure of the Photosphere

The solar oblateness (Section 1.2.5) and the limb-darkening function, as well as any large-scale structures in photospheric brightness, may vary systematically with the solar cycle. Observations now extend over 11 years, and contain over 2×10^{10} data points at the limb. This database is unique in several ways and represents a major contribution by RHESSI to our knowledge of solar global structure and variability, the underpinning of the solar dynamo action and all that we study. We believe that this capability should be extended as long as possible, and eventually replaced with a similar overlapping capability for future observations.

1.3.6 Science Goal 6 – Nonsolar Objectives

Researchers have begun to mine existing RHESSI data more deeply for new TGFs (Gjesteland et al. 2012); a new search algorithm in prototype has also found a larger population of events. While the rear segments of RHESSI's detectors are deteriorating in spectroscopic performance (see Section 2.2.1), this matters much less for TGFs than for other non-solar science, because the most useful characteristic of the TGF data at this point (Section 1.2.6.1) is simply the time and place of occurrence, from which the context data from lightning and meteorology can be used in the analysis for a given storm.

It must be noted that new TGFs to be discovered as the extended RHESSI mission progresses have a greater scientific value than events in the archive, because worldwide detection and analysis of lightning in the radio band continues to improve every year. TGF-associated lightning is detected with increasing efficiency globally by the World Wide Lightning Location Network (WWLLN; see, e.g., Gjesteland et al. 2011 for joint RHESSI/WWLLN results). The sensors run by Duke University provide even more detailed information about lightning/TGF connections, but only in the US/Central America/Caribbean/Atlantic region (Lu et al. 2011).

Now there are extensive TGF programs on Fermi and AGILE, and four other space missions are being prepared for launch over the next few years with detectors specifically intended for TGF studies: the French TARANIS, the European ASIM, and the US Firefly and Firestation. RHESSI has a higher-latitude orbit than the currently operating missions and can sample storms in non-tropical regions, providing a greater variety of meteorological context and therefore a better sense of the role of TGFs in different storm types.

1.4 Potential for Performance in the FY-14 to FY-18 timeframe

1.4.1 Relevance to the SMD Science Plan and contributions to HSO

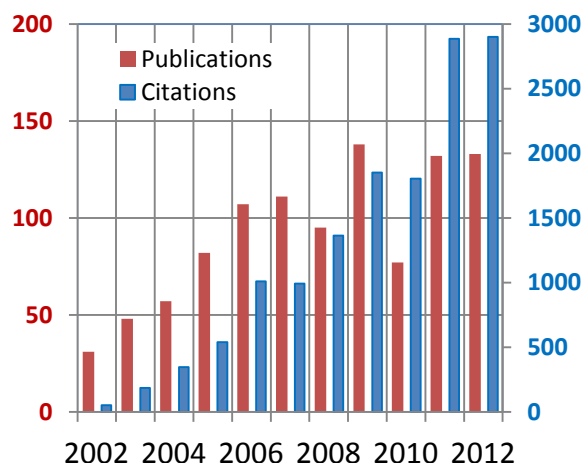


Figure 1-15. Number of refereed publications (red, left scale) per year that involve RHESSI and the number of citations per year to those papers (blue, right scale) (Q. Chen, private communication).

RHESSI is directly relevant to achieving NASA's strategic goal for Heliophysics to "Understand the Sun and its interactions with the Earth and the solar system." It addresses the SMD Science Question - "What causes the Sun to vary?" and the following Science Area Objectives: "Understand the fundamental physical processes of the space environment from the Sun to Earth" and "Maximize the safety and productivity of human and robotic explorers by developing the capability to predict the extreme and dynamic conditions in space."

1.4.2 Productivity and Vitality of Science Team

The first eleven years of RHESSI operations have been extraordinarily productive. To date, RHESSI observations have contributed to over 1,000 published papers and some fifty PhD and master's theses –

<http://www.lmsal.com/~aschwand/publications/rhessi.html>. The number of published articles and the citations per year taken from the NASA ADS web site are shown in Figure 1-15.

The current status of our understanding of solar flares recently appeared in a complete ~500-page volume of *Space Science Reviews* (Volume 159, 2011), subsequently published as a stand-alone book by Springer in 2012 entitled "High-Energy Aspects of Solar Flares." The nine

chapters of this work were written primarily by RHESSI-supported US scientists and international scientists who have made extensive use of RHESSI observations in their research. In the relatively short time since this volume was published, the papers have received over 100 citations.

The Max Millennium Program

The RHESSI PI team created and supports the Max Millennium program accessible at http://solar.physics.montana.edu/max_millennium/. It serves several functions that are key to the successful acquisition of observationally complete datasets and the full scientific exploitation of those observations. These functions include the daily recommendations of targets for joint observations and the establishment of joint observing plans with specific scientific goals in the event of predicted major flare activity.

RHESSI-supported Scientific Workshops

RHESSI personnel have initiated, organized, and attended many scientific meetings and special sessions, including twelve RHESSI-specific workshops and three multi-disciplinary workshops (Sonoma 2004, Napa 2008, Petaluma 2012). Various sessions have been held to educate the scientific community on how to use the RHESSI data analysis software in order to obtain the best possible images and spectra. Several international teams of scientists have also met under the sponsorship of the International Space Science Institute (ISSI) to explore issues related to RHESSI science. We will continue this sequence of scientific meetings.

Science Nuggets

Beginning in March 2005, the RHESSI team began a biweekly series of “Science Nuggets” at http://sprg.ssl.berkeley.edu/~tohban/wiki/index.php/RHESSI_Science_Nuggets. Each Nugget is a brief report that is intended to introduce various aspects of the scientific material to a technically competent audience. Both RHESSI team members and a worldwide community of interested scientists contribute to the Nuggets, now approaching 200 in number.

1.4.3 Data Accessibility and Usability

Full details of RHESSI data accessibility and usability are given in the accompanying Mission Archive Plan. The data archive contains the full Level-0 telemetry data, the RHESSI flare list, and quicklook lightcurves, spectra, images, and housekeeping plots for the entire mission. These plots, as well as context information discussed below, are easily accessed using the RHESSI Browser, <http://sprg.ssl.berkeley.edu/~tohban/browser/>. The archive, currently ~7 TB, resides on a private server at SSL and two public servers, one at Goddard and the other at FHNW in Switzerland.

Extensive RHESSI documentation is at <http://hesperia.gsfc.nasa.gov/rhessi/>, with comprehensive descriptions of the mission, the instrument, the science objectives, data analysis techniques, the software, and the data archive. In addition, support personnel are available at all three data sites to guide scientists in using the software and interpreting the results.

Software

One of the unique characteristics of RHESSI is that the telemetered data contain detailed information on each detected photon. This provides the flexibility to make *ex post facto* decisions and tradeoffs associated with time resolution, energy resolution, imaging resolution and field of view, etc., enabling the analyst to optimize these parameters as needed. Another advantage of this photon-oriented database is that ongoing improvements to the software and instrument calibration can be fully applied retroactively to all the data since the beginning of the mission.

The complete RHESSI software package necessary for the analysis of all RHESSI data is available online as part of the Solar Software (SSW) tree. It is written in the Interactive Data

Language (IDL); is compatible with Linux, Mac OS X, and Windows; and can be run via a combination of the IDL command line interface (CLI), a graphical user interface (GUI), or scripts. The software generates image cubes (in time and energy), spectra (either spatially-integrated or feature-specific), and light curves, and provides support for comparisons with data products from other missions (see below).

Spectral analysis capabilities are now enhanced by adding templates for the gamma-ray lines between ~300 keV and 10 MeV that depend on the spectrum, composition, and directionality of the accelerated ions, and the ambient solar abundance. Templates of pion-decay gamma-ray spectra extending to higher energies covered by Fermi GBM and LAT are also available.

Powerful visibility-based X-ray analysis can now be routinely carried out using several different image-reconstruction algorithms that include the capability to compute spectrally regularized image cubes. Visibilities are calibrated, instrument-independent, Fourier components of the source image. Mathematically, they correspond to the output of a single baseline of a radio interferometer. For RHESSI, they represent an intermediate data product directly obtained from the observed time-modulated light curves. The basic visibility software has enabled the accurate determination of HXR source sizes (useful for example to convert thermal emission measurements to electron densities), and the evaluation of albedo; it was the computational tool of choice in obtaining several of the recent results discussed above. The ESA-funded High Energy Solar Physics in Europe (HESPE) project is compiling a complete set of visibility-based data spanning the duration of the RHESSI mission, thus allowing the essential imaging spectroscopy information to be encoded very compactly.

Facilities for Multi-wavelength Analysis

The following steps have been taken to support the convenient integration of RHESSI data into studies involving other wavelength regimes:

- The RHESSI software package includes flexible tools for accessing and integrating multiple data sets (e.g. overlaying images). Coalignment is simplified since the absolute positions of RHESSI images are inherently determined to arcsecond accuracy.
- The Synoptic Data Archive at the GSFC Solar Data Analysis Center (SDAC) provides access to image, spectral, and lightcurve datasets spanning a broad wavelength range from radio to gamma-rays. Datasets from spacecraft include - SDO; STEREO; Hinode; SOHO; TRACE; SOXS; GOES; and FERMI. Data sets from ground observatories include - BBSO, Meudon, Kanzelhoehe, Kiepenheuer, Callisto, Phoenix, OVSA, Nobeyama, and Nancay. The Synoptic archive is integrated with the Virtual Solar Observatory (VSO), using common IDL tools to import complementary observations into the RHESSI data analysis software.
- SDO/AIA cutout image FITS files and movies are generated for every RHESSI flare observed after September 2010. These movies are linked from the RHESSI Browser, and the FITS files are available through the Synoptic Data Archive mentioned above.
- Science-ready RHESSI time profiles, images, and spectra conforming to SPASE guidelines are now being generated for each event. They will be accessible from the RHESSI Browser, through the VSO (and therefore the Synoptic Archive), and in (J)Helioviewer.
- The spectral analysis software package written for RHESSI also handles X-ray and gamma-ray data from Fermi, MESSENGER, and SOXS, allowing users to analyze these different data types in a familiar environment

Browser

The RHESSI web-based Browser is available at the following location:

<http://sprg.ssl.berkeley.edu/~tohban/browser/?show=grth+qlpcr>

It provides a quick and easy way to display the wealth of RHESSI quicklook plots and complementary plots from other instruments. Many batch processes run autonomously to

produce the available quicklook plots of RHESSI lightcurves, images, detector monitor rates, and more. In addition, quicklook plots of context observations are autonomously generated and archived, including GOES, Fermi GBM and LAT lightcurves, SDO AIA movies, and various WIND/WAVES and NRH radio plots.

Browser is a powerful tool that allows the user to load a variety of plots relevant for a specified time, and then easily step back and forth through time as desired. To investigate the context of RHESSI events, Browser also dynamically generates links for the selected time to other databases, including SolarMonitor.org, Helioviewer.org, and the SDO AIA cutout movies discussed above.

1.4.4 Promise of future impact and productivity

RHESSI is still fully operational and shows tremendous promise for the coming years of maximum solar activity and joint observations with the newer solar missions now in orbit. RHESSI continues to be the only mission capable of solar HXR imaging spectroscopy and is likely to retain that unique position until the launch of the Spectrometer Telescope for Imaging X-rays (STIX) on the European Solar Orbiter with a nominal start of science observation in 2020. RHESSI's gamma-ray imaging spectroscopy capabilities are unlikely to be matched for many years. Thus, it is critical that RHESSI be available for as long as possible to provide the high-energy coverage of the flares that will be seen with the advanced instrumentation on Hinode, STEREO, SDO, and Fermi, and the improved ground-based radio and optical observatories such as EOVSAs.

The long-term prospects for the RHESSI germanium detector performance are discussed in Section 2.2.1. In summary, we expect that a fourth anneal will be needed sometime in 2014 and that operations can continue well into 2018, with some reduction in performance but with the core HXR imaging spectroscopy capability retained.

2 TECHNICAL AND BUDGET

2.1 Spacecraft

RHESSI was launched on February 5, 2002, into a circular orbit with an altitude of 600 km and an inclination of 38°. The observatory continues to function very well after 11 years of operations in its present 554 x 533 km orbit. All of its subsystems are fully operational. RHESSI has no expendables and the relatively low level of solar activity means that its orbital decay has been less than predicted. The latest orbital lifetime predictions made by Flight Dynamics Support Services (Code 595) at Goddard show that the "Mean Nominal" predicted reentry date is 28 November 2023 and the "Early +2 Sigma" date is 31 August 2018. Consequently, RHESSI's useful life should extend at least into 2018.

The solar array power output has declined slightly since launch but the battery voltage and absolute and differential pressures have been relatively stable for the past 3 years. The solar arrays and the battery are projected to continue providing adequate power generation and storage. The average spacecraft temperature has increased by only ~1° C since launch. The S-band transceiver still generates a stable output power of 5 W with clean BPSK modulation at 4.0 Mbps, and the receiver shows no signs of deterioration in performance. The attitude control system is stable and the C&DH subsystem shows no signs of degradation.

The telecommunications subsystem has generally been stable since launch. However, following the detector annealing in November 2007, the receiver is seeing increased noise from the spacecraft power bus, and ATS table loads are unsuccessful during nighttime passes. This situation is easily mitigated by scheduling daylight passes at the Santiago ground station during infrequent periods when both the Berkeley and Wallops ground stations have only nighttime passes.

On March 16, 2010 the spacecraft experienced a power related anomaly. It appears the hardware under-voltage (UV) protection tripped and turned off all spacecraft loads that are not connected to the essential bus, and set the battery V/T charge level to the lowest setting (0). With all heaters turned off, the battery temperature dropped to at least -36 C, at which temperature it performs very poorly, causing a brown-out on the essential bus. This resulted in negative acquisitions and difficulty waking up the spacecraft. The spacecraft was fully recovered on May 1, 2010, including annealing the detectors, and all onboard systems that could have caused a power problem have been checked out. Since the anomaly occurred, spikes have been detected in the telemetry, and one such spike caused an over-current (OC) trip on Non-Essential Bus 1 (NEB1). All indications are that this OC trip was spurious. A similar spike could have caused the UV3 trip to shut off all loads and set all switches to zero position, which was the state of the spacecraft when telemetry was restored. The source of the spikes has not been identified, but the Flight Operations Team continues to monitor the situation.

To prevent a recurrence of this anomaly, the decision was made – with concurrence of the Space Science Mission Operations (SSMO) Project at NASA/GSFC and the Systems Engineer at Orbital Science Corporation – to disable all over-current and under-voltage hardware trip circuits, as well as the over-current and battery under-pressure protection in the flight software. The risk associated with disabling the on-board fault detection and correction system was assessed to be lower than the risk of losing the cryocooler or the germanium detectors in case of a recurrence of the anomaly.

Aside from the described problems, all other subsystems and sensors are functioning nominally. Overall, there is no reason to believe that the spacecraft will not continue to function very well over the next several years.

2.2 Instruments

2.2.1 Spectrometer and Cryocooler

The RHESSI germanium spectrometer and its Sunpower cryocooler continue to provide excellent performance. The cryocooler has operated nearly continuously for more than 100,000 hours. While showing signs of degraded performance, it is continuing to operate with an input power of 70 watts and negligible microphonics. The detector temperature has increased from about 74 K to 110 K over the course of the mission, but the detectors should continue to operate effectively all the way up to 150 K, at which point bulk conductivity of the germanium begins to introduce a problematic leakage current. At the current rate of temperature increase of ~8 K per year, this point would not be reached until 2018.

RHESSI's germanium detectors are each in the shape of a cylinder with a small central bore that runs from the bottom up to about 1 cm from the top. Although each detector consists of a single crystal of pure germanium, it is divided electrically into two segments. The front ~1.5-cm thick segment is read out through one electrical contact at the top of the inner bore and the rear ~7 cm through another contact further down the bore. This is accomplished by lining the bore with a conductive contact of diffused lithium ions that is interrupted about 1 cm from the top end of the bore. The front segment stops most hard X-rays below ~200 keV, and is used for X-ray science down to ~3 keV, while the rear segment registers gamma rays above ~100 keV, in particular in the nuclear line region. The vast majority of flares observed by RHESSI are studied primarily using front-segment data; only a small fraction of M-class flares and perhaps half of all X-class flares produce gamma-ray emission that enables use of the rear segments.

Radiation damage from encounters with radiation belt protons in the South Atlantic Anomaly gradually degrades the energy resolution of RHESSI's detectors, and, when it advances to an extreme degree, renders the outer cylindrical layer of the detector volume completely insensitive to interactions. Three times over the course of the mission, in November 2007, April 2010, and

February 2012, RHESSI's germanium detectors were annealed to reverse the effects of radiation damage resulting in the recovery of high energy resolution and sensitive volume. In this procedure, the coldplate to which they are mounted is heated to $\sim 100^\circ\text{C}$, causing the crystals to reach a similar temperature. While this does not actually cause atoms to move in the lattice and "heal" the disordered regions produced by proton and neutron interactions, it renders these disordered regions unable to trap moving holes in the crystal, and therefore neutralizes them in terms of their effect on detector performance.

Unfortunately, these periods of high temperature also cause the lithium ions that make up the inner contact to drift in the crystal, eventually shorting out the separation between the front and rear segments. An unsegmented detector has higher background (incorporating, as it does, both the front and rear detector volumes), broadened energy resolution (typically $\sim 10\text{ keV}$ FWHM at 100 keV as opposed to $1\text{--}2\text{ keV}$ for a segmented detector), and an elevated threshold ($\sim 20\text{ keV}$ vs. 3 keV for a segmented detector). Unsegmented detectors can still be used for RHESSI's core observational capability of imaging spectroscopy above $\sim 20\text{ keV}$ with no loss in angular resolution or sensitivity to events well above background. Calculations and laboratory experiments with a spare germanium detector predicted that the third anneal would have some chance of affecting the ability for individual detectors to segment. This was borne out when two of the nine detectors lost segmentation following that anneal. After waiting for radiation damage to accumulate, which can actually act to aid segmentation, segmentation has been restored in one of these detectors by raising the high voltage above the nominal $4,000\text{ V}$. We are attempting to do the same with the other detector as of this writing.

A fourth anneal may well desegment other detectors, possibly irreversibly, so we pay particular attention to the scientific capabilities of RHESSI with all the detectors unsegmented. We find that hard X-ray imaging above 20 keV is virtually unaffected except for the weak flares where the increased background becomes an issue. Figure 2-1 shows images of a flare from 2012 July 19 made with five RHESSI detectors, those under grids 1, 2, 3, 4, and 5. The detectors under grids 1, 3 and 5 are segmented and those under 2 and 4 are the two that became unsegmented in the third anneal. Aside from the changes in the apparent source sizes – due to the increasing pitch of the grids over each detector – the images are all of comparable quality. Also, the best-fit power-law index (γ) has the same value within uncertainties for all detectors, independent of their segmentation status. This demonstrates that after desegmentation of all detectors, RHESSI will continue making what is probably its most

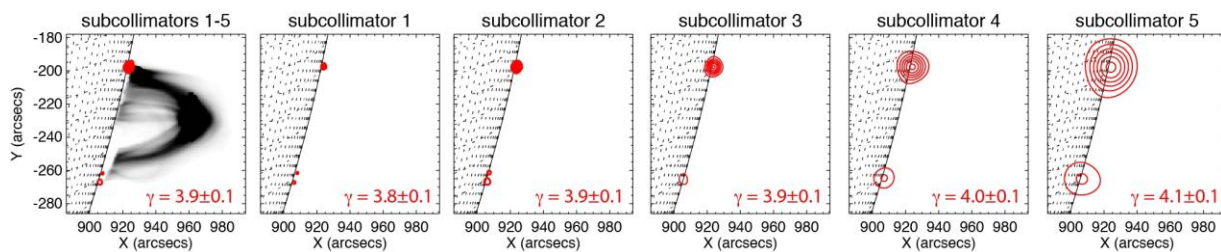


Figure 2-1. Imaging footprints at $35\text{--}80\text{ keV}$ during a flare on 2012 July 19 with RHESSI's five finest grids. The image quality and the best fit power-law spectral index (γ) using the unsegmented detectors (#2 and #4) are unaffected. The background image in the first panel is from SDO/AIA at 131 \AA .

important contribution in the mature phase of its mission: revealing the sites of high-energy electron interactions in flares that are studied across wavelengths by a variety of spacecraft and ground-based instruments. Imaging spectroscopy will still be possible in relatively broad energy bands above the $\sim 20\text{ keV}$ threshold. For example, energy bins of $20\text{--}30\text{ keV}$ and $50\text{--}70\text{ keV}$ could still provide cleanly separated images of superhot thermal emission and nonthermal emission in a large flare.

Based on the current state of radiation damage, and the history after the previous anneals, we should maintain the ability to see nuclear lines in the rear segments until about the end of 2013, and have drastically reduced effective area in the front segments by mid-2014. When we feel the front segment performance is compromised enough that annealed but unsegmented detectors would be preferable, we will perform the fourth anneal, probably around late 2014. A fifth or sixth anneal will also be possible as long as the cryocooler continues to degrade gracefully, thus extending RHESSI's useful life to 2018.

2.2.2 Imager

The RHESSI imager subsystem consists of nine rotating modulation collimators, each of which has a pair of widely separated grids. A metering structure maintains the relative twist alignment of the nine grid pairs. The imaging subsystem is inherently stable and has shown no evidence of change in grid alignment. Improved analysis techniques are refining the calibration of the grid parameters and locations (now known to submicron accuracy), the results of which are built into the software package and are applicable to all data acquired since launch.

2.2.3 Aspect System

There are three parts to the RHESSI aspect system. The absolute pitch and yaw angles relative to Sun center are provided by the Solar Aspect System (SAS), with sub-arcsecond accuracy. The roll angle is provided by two redundant side-looking star scanners, a CCD-based Roll Angle System (RAS) and a PhotoMultiplier-Tube-based Roll Angle System (PMTRAS).

The SAS consists of a set of three identical lens/sensor subsystems, each of which focuses a narrow-bandwidth image of the solar disk onto a linear CCD array. No anomalies in its operation have been observed. During the first few months of the mission, the sensitivity of the SAS decreased, but it has now stabilized at ~60% of the original value, a level which provides an order-of-magnitude sensitivity margin with no compromise in accuracy. The SAS also continues to provide the most accurate solar radius measurements ever made, for the study of global solar applications as discussed in Section 1.2.5. We now operate this instrument in campaign mode to obtain much larger data bandwidths during special conditions, such as RHESSI anneal operations or SDO roll maneuvers (these are the twice-yearly times when SDO can get comparable global imaging information).

The PMT-RAS continues to provide the roll aspect knowledge upon which most of the solar imaging is based. Its response has remained stable since launch, easily meeting the 1 arcminute roll-angle requirement with a large margin in sensitivity.

The CCD-based RAS has also proven to be stable and able to meet the same roll-angle requirement. CCD-RAS data are used to fill occasional gaps in the PMT-RAS coverage. In addition, by measuring the polar angle as well as the roll angle, the CCD-RAS can provide full aspect information with 10 arcsecond accuracy for non-solar targets such as the Crab Nebula and the pulsar A0535+26.

As described above, the SAS data (with the help of RAS and PMT-RAS) produce valuable and unique science that is outside the primary goals of RHESSI: the characterization of the shape and brightness of the solar photosphere at the highest levels of precision (see Sections 1.2.5 and 1.3.5). This application becomes all the more important as the mission life increases because these precise measurements can be applied to solar-cycle variations.

2.3 Ground System

In 1999, a multi-mission operations facility was established at SSL to support the RHESSI and FAST missions. The joint facility, which now also supports other missions, includes the Mission Operations Center (MOC), the Science Operations Center (SOC), the Flight Dynamics Center (FDC), and the Berkeley Ground Station (BGS). A high degree of integration and

automation combined with flexible system architecture provides a reliable and cost-effective state-of-the-art environment to perform all functions required to operate multiple spacecraft simultaneously.

2.3.1 Ground Stations

The primary ground station for the RHESSI mission is BGS. It consists of an 11-m parabolic reflector mounted on a pedestal with a three-axis drive system, and an S-band RF system. BGS operations have been very reliable, supporting more than 50,000 passes for RHESSI, FAST, CHIPS and THEMIS combined. Backup support is provided by Wallops Island (WGS), Santiago (AGO), and the DLR ground station at Weilheim, Germany. BGS has supported more than 21,000 RHESSI passes since launch - 5-6 passes per day on average. WGS and AGO support typically 4 passes per day combined. The average daily data volume is 13.5 Gbits with an overall telemetry recovery efficiency of ~99%.

2.3.2 Mission Operations Center

The RHESSI Mission Operations Center is part of a secure, shared state-of-the-art facility with a network of workstations for flight dynamics, spacecraft command and control, mission planning, command load generation, and data trending. The facility, typically staffed during normal working hours only, performs automated pass supports, spacecraft and instrument state-of-health checks, and generation of all ephemeris and planning products in a lights-out mode.

RHESSI normal operations comprise mission planning functions, command load generation, real-time pass supports, spacecraft state-of-health monitoring, data trending, instrument configuration, and science data recovery and archiving. Generation of all ephemeris and mission planning products is based on two-line element sets that are downloaded from the Space-Track.org web site, quality checked and archived locally in a fully automated mode. Spacecraft ATS loads are built by the Flight Operations Team (FOT) and uploaded to the spacecraft multiple times per week. Every six weeks, the spacecraft is spun up from about 14.5 rpm to its nominal spin rate of 15 rpm. The FOT works closely with project scientists to determine the optimal instrument configuration consistent with the current level of solar activity. During off-hours, FOT members are automatically notified by cell phone regarding any spacecraft or ground system anomalies. A number of web-based tools allow FOT members, subsystem engineers, and instrument scientists to remotely monitor spacecraft and instrument performance.

Since RHESSI is operated from a multi-mission facility, its resources are shared with other missions. This approach provides redundancy and reduces overall operations costs. The flight control team now operates RHESSI, the 3-spacecraft THEMIS constellation (THEMIS A, D & E), 2 ARTEMIS spacecraft (formerly THEMIS B & C) in lunar orbits, the NuSTAR SMEX mission and the NSF CubeSat CINEMA – both launched in 2012 – for a total of 8 spacecraft.

2.3.3 Science Operations Center

The RHESSI SOC, located at SSL, consists of a RAID server, with ~13.7 TB of data capacity, and six processors. The SOC receives RHESSI data after every ground-station contact and automatically processes them to create Level-0 data files. As of March 2013, there are ~95,000 Level-0 files, containing 7 TB of data, for an average of 1.8 GB per day.

Other automated procedures generate quick-look data containing the RHESSI observing summary, flare list, and quick-look light curves, images, and spectra. Long-term trend plots of SOH data are updated daily in the SOC. All of these data products are available through the RHESSI website - <http://hesperia.gsfc.nasa.gov/rhessi/>.

2.4 References

- Allred, J. C. 2005, PhD thesis, U. Washington
Allred, J. C., et al. 2005, *ApJ*, 630, 573
Aurass, H., et al. 2013, *A&A*, submitted
Bain, H. M., & Fletcher, L. 2009, *A&A*, 508, 1443
Battaglia, M., & Benz, A. O. 2009, *A&A*, 499, L33
Baylor, R. N., et al. 2011, *ApJ*, 736, 75
Bellm, E. C. 2010, *ApJ*, 714, 881
Berkebile-Stoiser, S., et al. 2009, *A&A*, 505, 811
— 2012, *ApJ*, 753, 88
Brosius, J. W., & Holman, G. D. 2010, *ApJ*, 720, 1472
Caspi, A., et al. 2013, in preparation
Chen, B., et al. 2013, *ApJ*, 763, L21
Chen, Q., & Petrosian, V. 2012, *AAS Abstract #220, #204.25*
Christe, S., et al. 2011, *Sol. Phys.*, 270, 493
Dickson, E. C. M., & Kontar, E. P. 2012, *Sol. Phys.*, 301
Dwyer, J. R., et al. 2010, *JGR*, 115, 9206
Emslie, A. G., et al. 2004, *JGR*, 109, 10104
— 2005, *JGR*, 110, 11103
— 2012, *ApJ*, 759, 71
Fivian, M. D., et al. 2008, *Sci.*, 322, 560
Fleishman, G. D., & Kontar, E. P. 2010, *ApJ*, 709, L127
Gjesteland, T., et al. 2011, *JGR*, 116, 11313
— 2012, *GRL*, 39, 5102
Glesener, L., et al. 2012, *ApJ*, 754, 9
— 2013, in preparation
Guo et al. 2013, *ApJ*, 766, 28
Hannah, I. G., et al. 2010, *ApJ*, 724, 487
Hannah, I. G., & Kontar, E. P. 2012, *A&A*, 539, 14
Holman, G. D. 2003, *ApJ*, 586, 606
— 2012a, *Phys. Today*, 65, 56
— 2012b, *ApJ*, 745, 52
Hudson, H. S. 2007, *ApJ*, 663, L45
Hurford, G. J., et al. 2006, *ApJ*, 644, L93
— 2003, *ApJ*, 595, L77
Inglis, A., et al. 2012, *AAS Abstract*, 220, 509.05
Kaufmann, P., et al. 2004, *ApJ*, 603, L121
Klimchuk, J. A. 2006, *Sol. Phys.*, 234, 41
Kontar, E. P., & Brown, J. C. 2006, *ApJ*, 653, L149
Kontar, E. P., & Reid, H. A. S 2009, *ApJ*, 695, L140
Kowalski, A. F., et al. 2012, *Sol. Phys.*, 277, 21
Kretzschmar, M. 2011, *A&A*, 530, A84
Krucker, S., et al. 2007, *ApJ*, 669, L49
— 2008a, *A&A Rev.*, 16, 155
— 2008b, *ApJ*, 681, 644
— 2010, *ApJ*, 714, 1108
— 2011, *ApJ*, 742, 82
— 2013, *A&A Rev.*, in press
Kuhn, J. R., et al. 2012, *Sci.*, 337, 1638
Landi, E., et al. 2010, *ApJ*, 711, 75
Lin, R. P., et al. 2002, *Sol. Phys.*, 210, 3
— 1984, *ApJ*, 283, 421
Liu, W., et al. 2009, *ApJ*, 693, 847
Liu, W., et al. 2013, *ApJ*, in press
Lu, G., et al. 2011, *JGR*, 116, 3316
Luethi, T., et al. 2004, *A&A*, 415, 1123
Martinez Oliveros, J. C., et al. 2012, *ApJ*, 753, L26
Masson, S., et al. 2009, *Sol. Phys.*, 257, 305
Milligan, R. O., et al. 2012, *ApJ*, 748, L14
Murphy, R. J., et al. 2009, *ApJS*, 183, 142
Omodei, N., et al. 2012, *AAS Abstract* 220, 424.03
Petrosian, V. & Chen, Q. 2010, *ApJ*, 712, L131
Piana, M., et al. 2003, *ApJ*, 595, L127
Prato, M., et al. 2009, *ApJ*, 706, 917
Reames, D. V. 2013, *Space Sci. Rev.*, online
Ripa, J., et al. 2012, *ApJ*, 756, 44
Ryan, J. 2000, *SSR*, 93, 581
Saint-Hilaire, P., et al. 2010, *ApJ*, 721, 1933
Schrijver, C. J., et al. 2012, *JGR*, 117, 8103
Share, G. H., et al. 2003, *ApJ*, 595, L85
— 2004, *ApJ*, 615, L169
Shih, A. Y., et al. 2009, *ApJ*, 698, L152
— 2011, *AAS/SPD Abstract #42*, 2205
Smith, D. M., et al. 2003, *ApJ*, 595, L81
Su, Y., et al. 2011, *ApJ*, 731, 106
— 2013, *Nature Phys. Sci.*, submitted
Torre, G., et al. 2012, *ApJ*, 751, 129
White, S. M., et al. 2011, *Space Sci. Rev.*, 159, 225
Woods, T. N., et al. 2004, *GRL*, 31, 10802
Zharkova, V. V., et al. 2011, *Space Sci. Rev.*, 159, 357

APPENDICES

3 EDUCATION AND PUBLIC OUTREACH

Quality, Scope, Realism, and Appropriateness & Resource Utilization

This program will add RHESSI data at the entry level of Goddard’s Space Weather Action Center (SWAC), add awareness of RHESSI science and support teachers’ engagement in the Heliophysics Educator Community of Practice (HE CoP), and increase the public’s awareness of the Sun and space sciences at the Open House at the Space Sciences Laboratory (SSL) at UC Berkeley (Cal Day) and other outreach events. All of these programs are supported by multiple missions so minimal costs are involved in sharing RHESSI’s unique findings of the Sun in these customer-focused educational and outreach programs. The program will be run as a collaborative program between the Heliophysics Science Division at Goddard taking the lead for SWAC and SSL at UC Berkeley taking the lead for the HE CoP and Cal Day.

There is evidence from past RHESSI and other NASA mission education efforts that exposing teachers and students directly to the RHESSI/NASA mission data is an effective and positive mode of engagement. Through SWAC and the RHESSI magnetism guide, which was developed many years ago and is now accessible via <http://nasawavelength.org>, the RHESSI data goes beyond the scientific community and is used to teach scientific practices while also educating students about solar physics. As the K-12 Framework (NRC, 2011) is now being implemented into national science education standards, effective means to teach scientific practices will become more of a focus. NASA is thus poised to help the nation learn these practices through types of educational programs that use NASA’s science data, such as this proposed RHESSI E/PO effort.

Objectives

Objective	Outcome
Utilize SWAC to give educators access to RHESSI data and provide educators additional heliophysics knowledge through professional development activities	Web training through HEA and SED where educators learn heliophysics and analyze RHESSI data
Identify and promote increased interest in heliophysics and provide the means to pursue these interests in education environments	A communication place for educators to meet with colleagues to teach and learn heliophysics
Promote diverse under-represented audience participation in heliophysics programs	Sharing heliophysics resources with partners reaching diverse audiences
Increase informal audiences’ awareness of the Sun and space science careers by providing NASA content, specifically in heliophysics, at Cal Day and other outreach events	Resources are available to others wanting to learn more about heliophysics through Sun-Earth Days and SWAC

Goals

1. Inspire and inform educators about the dynamic science of the Sun, its influence on Earth and space environments in a communication environment that keeps them connected with each other and the content providers (via a “community of practice”)
2. Engage teachers and students in RHESSI science by adding a RHESSI data component to the SWAC program for use in heliophysics STEM education and outreach

3. Provide high-quality professional development opportunities and facilitated discussions through WebEx for Heliophysics Educator Ambassadors (HEA) and Sun-Earth Days (SED) educators using NASA's unique missions and research through SWAC
4. Engage San Francisco Bay Area families in solar science and careers in space science at the open house day at the University of California, Berkeley (Cal Day)

NASA Space Weather Action Centers (SWAC) (<http://sunearthday.gsfc.nasa.gov/swac/>)

SWAC represents a new approach to teaching science and technology in classrooms. Students are encouraged to act like real scientists by accessing, collecting, analyzing, recording, and communicating space weather forecasts. Imagine being able to predict and monitor the progress of a massive solar storm from the time it erupts from the million degree solar corona until it sweeps past our small planet effecting enormous changes in our magnetic field and impacting life on Earth in a variety of ways. The SWAC web-based portal, shown below, replicates the operational functions of the NOAA Space Weather Prediction Center in providing access to NASA mission science results, observation techniques, and analysis methods used by scientists. The ALERT is created as “nightly” news reports on space weather that predicts impending effects on Earth.



RHESSI X-ray quick-look light curves and images are already accessible from the SWAC web site. An ongoing project will allow students to overlay improved X-ray images of flares on images at other wavelengths (e.g., SDO/AIA movies). These combined images will show the location of the flare-accelerated electrons that produce the

X-rays in relation to the flare-heated plasma that emits in the EUV imaged with AIA. The resulting movie will be accessible by students for use in their “news report,” with the inevitable delay of a day or so before RHESSI’s data is telemetered to the ground.

Through the SWAC program, participants quickly learn how to create ‘easy to make’ space weather “learning centers” in the classroom that allow them to monitor and report the progress of a solar storm. SWAC is an extremely robust learning tool complete with step-by-step tutorials on how to interpret ‘near real time’ heliophysics data from 10 missions and 36 instruments. Teacher input confirmed that in order for SWAC to be integrated into the classroom environment, introductory steps were required to enable student users to become familiar with the basic steps needed to comfortably increase comprehension. As a result, the SWAC program was further designed with data links and tutorials needed to monitor the progress of a solar storm from the time it erupts from the Sun until it sweeps past the Earth.

Cal Day – Open House at the Space Sciences Laboratory at UC Berkeley

RHESSI E/PO funding will also support the planning and implementing of a public outreach event at SSL in 2014 and 2015. This already established, once-a-year event, called Cal Day, includes free tours of the lab, a special program in the Mission Operations Center where satellites are monitored, science talks about on-going space missions (including STEREO), a career panel, multiple booths with related fun hands-on activities, a solar telescope, and more (<http://cse.ssl.berkeley.edu/calday/>). **In 2010, 2011, and 2012, Cal Day attracted 350, 500, and 500 participants, respectively.** In the written evaluations collected, over 97% of the respondents stated that the event was a good use of their time, and a higher percentage said they would recommend it to a friend. Some notable quotes were “It was incredibly cool. I came for my science class and learned a bunch”, “I was able to learn more about space and the Sun”, “...the career panel and black hole lecture were great”, and “It was really interesting. I got to hear about NASA projects I didn’t know about”.

Partnerships/Sustainability (includes leveraging resources, networks, etc.)

The RHESSI E/PO program leverages several existing and proven programs built with collaborations across institutions and missions. *Sun-Earth Days* began in 2001 with an audience of 9000 and has grown each year with millions taking part during events such as eclipses and transits (**over 500 million participants world-wide for the Transit of Venus in 2012**). SWAC was established in 2003 as a component of Sun-Earth Days. It has gone through 4 revisions based on educator input; currently involved are **3000 educators world-wide and the Challenger Center network**. The *Heliophysics Educator Ambassador (HEA)* program focuses on in-depth learning experiences around Earth, Space, and Physical Science topics for **90 core educators teaching in middle and high school grades as well as teaching their peers**. The goal of the HEA program is to develop the capacity and provide the opportunity for educators to train other teachers on NASA Heliophysics science and educational resources. The program provides educators with a week-long training and follow-up support for several years via teleconference calls and other electronic communications. **Educators showed gains in knowledge of and confidence in teaching Heliophysics.**

We will continue to provide online and onsite training to students and teachers with heliophysics system science as HEA moves towards a deliberate 'Community of Practice (CoP)', an effort supported by the NASA Science Mission Directorate Heliophysics Science Education and Public Outreach Forum and funded by many NASA Heliophysics mission E/PO programs. CoPs are groups of people who share a concern, a set of problems, or a passion about a topic, and who deepen their knowledge and expertise in this area by interacting on an ongoing basis (Wenger, E., 1998). In this case, the people involved are middle and high school teachers who have been a part of individual mission E/PO education programs and networks, such as HEA. They are teachers who want to deepen their heliophysics content knowledge, increase their STEM teaching skills, support their students in learning STEM, and interact with other heliophysics educators. Members of a CoP self-select to be a part of it and they share their experiences and knowledge in a free-flowing way. Throughout FY14-FY18, activities in the CoP may include online discussion boards, in-person meetings (as budgets permit), webinars/online tagups, an email list-serv and/or a newsletter. In addition to supporting learning about the Sun through this CoP, RHESSI will also ensure that the Sun-Earth Day packets of products developed by missions, and approved through the annual NASA Product Review are shared with these teachers.

The SWAC and HE CoP utilize "multimission" approaches to E/PO activities encouraged by the Heliophysics Division to emphasize the "system-science" of heliophysics. In the SWAC, the videos, audio podcasts, and science content are designed to emphasize the interconnection of the Sun, solar wind, magnetosphere, and ionosphere; the prominence of the plasma state and plasma physics in these regions; and the effects of geomagnetic activity on the human experience on Earth. The Sun-Earth Days program is featuring an audio podcast series in 2013 about the RHESSI mission and data. There is also an education activity in which students use the podcasts to answer the question: *What can I learn from physics?*

Connections to Other NASA E/PO Activities

The benefit of working in collaboration with multiple mission E/PO projects and programs, is the ease in which one program can point educators, students and the public to other NASA E/PO activities. We will advertise other Science Mission Directorate SMD E/PO opportunities to the educators and students in our programs so that they may continue their learning of NASA's rich science through multiple educational engagements across SMD.

Evaluation (including outcomes and metrics)

As these programs are on-going programs, they have been evaluated in their ability to meet similar stated goals and objectives as in this proposal. Throughout this proposal, outcomes and

metrics are emphasized in italics in the areas describing each program. Note that the metrics have been entered into NASA’s Office of Education Performance Measurement (OEPM) and RHESSI E/PO plans to continue to enter metrics into OEPM in the following 5 years.

The evaluation of SWAC will be completed through Sun-Earth Day based on the evaluation for the Space Weather Action Center. The theme for 2013 is Solar Max-Storm Warning and the featured activity for formal education is the Space Weather Action Center. RHESSI data and the training will be included as part of the evaluation. The evaluation for the CoP will be a joint venture across Heliophysics Missions. The evaluation for Cal Day will build on past Cal Day evaluation questionnaires.

Objective	Metrics
Utilize SWAC to give educators access to RHESSI data and provide educators additional heliophysics knowledge through professional development activities	Survey to determine effectiveness of training for classroom use. Indicator: for success exceeding 90%
Identify and promote increased interest in heliophysics and provide the means to pursue these interests in education environments	Educators will use the communication center to ask questions, share their ideas and successes and failures. Indicator: frequent use in communication center
Promote diverse under-represented audience participation in heliophysics programs	Indicator: use of SWAC and the communication Center.
Increase informal audiences’ awareness of the Sun and space science careers by providing NASA content, specifically in heliophysics, at Cal Day and other outreach events	Web stats for SWAC would be expected to increase over previous years. Indicator on Cal Day: questionnaires of continued awareness of the Sun and space science careers.

Customer Needs Focus

With the *Framework for K-12 Science Education* that was released by the National Research Council (NRC) in July 2011 and the Next Generation Science Education Standards in draft form, “Teachers will need to reorganize instruction to emphasize fewer ideas and develop strategies for integrating content, science and engineering practices, and crosscutting themes.” (Penuel and Fishman, 2012) SWAC will help teachers teach scientific practices. Its use of scientific practices has already shown to make abstract concepts more concrete. Students are the essential workers in the educational process. They construct, discover, and develop central concepts. They create and solve problems. They read, write, talk, think, pose questions, and solve problems. They observe and manipulate aspects of their environment, and in the manipulation, confront problems about which they think, talk, write, and read. They take risks. These are the types of skills that the NRC, 2011 report indicates students need in order to learn science. Through SWAC, students exhibit understanding of the central concepts and competence with the essential skills in a problem-solving environment. Students exhibit competence in individual and group problem solving. Students exhibit a willingness to accept different kinds of solutions to the same problem and become lifelong learners with a focused interest in STEM content and discovery.

At the Summer 2012 HEA reunion workshop, teachers indicated during a focus group discussion a desire and need for continued engagement in teaching heliophysics to their students and peers. During FY13, 12 CoP lead teachers were selected from several teacher

networks associated with NASA SMD heliophysics missions (THEMIS, RHESSI, Van Allen, and other missions associated with the HEA program). These teachers and the heliophysics mission E/PO staff will meet during FY13 to shape the design of the CoP and invite teachers from all NASA Heliophysics E/PO teacher networks to participate in the CoP. Funding for this initial effort exists through FY13. The CoP will continue to be coordinated through FY'18.

Content (NASA-related and STEM/science education benchmarks/standards)

The goals of RHESSI E/PO align with the NASA Heliophysics Roadmap to collaborate with and engage educators to enhance their knowledge of heliophysics-related subjects and activities. By extension, the goals also support efforts to engage students and stimulate their interest in heliophysics-related STEM subjects. By training educators through enhanced professional development directly related to NASA Heliophysics missions, including RHESSI, through SWAC and the CoP, students will be better informed about STEM disciplines and the diverse range of career opportunities related to heliophysics science and missions.

The goals support NASA Education goals outlined in the President's 2011 budget to immerse students and educators in current NASA science and technology, with increasing emphasis on e-Education and cyber learning opportunities. The proposed professional development opportunity will enable teachers to better motivate students to achieve academic excellence and pursue STEM careers thus meeting the following AAAS Benchmark 2061:

Technology is essential to science for such purposes as access to outer space and other remote locations, sample collection and treatment, measurement, data collection and storage, computation, and communication of information. (3A/M2) As mentioned above, this proposal effort also ties in directly with the NRC (2011) K-12 Framework recommendations of emphasizing scientific practices. In the Next Generation Science Education Standards, sunspots are specifically called out as a scientific topic

Pipeline

Teaching Heliophysics through the SWAC and CoP initiatives will promote discovery and exchange of knowledge and ideas through collaboration and classroom teaching. Past experience and evaluation findings have provided some evidence from teachers that supporting the HEAs and Educators involved in Sun-Earth Days allows these teachers to provide students with learning experiences that excite the students about physics, the Sun, space weather, and the use of data in their learning. Teachers have indicated that ensuring RHESSI resources are aligned with standards, including the Common Core standards, will academically allow teachers to justify their inclusion of RHESSI resources in their classrooms. Teachers have also indicated in evaluation of the HEA program and SWAC that utilization of NASA data, and participation and input of STEM researchers, helps to teach students how to think outside of the 'fact-based' science paradigm and learn scientific practices. RHESSI's E/PO program will continue to support such important pipeline impacts that come from multi-mission collaboration in education efforts.

Diversity

The changing demographics of our country make it imperative that the science community in general and NASA in particular, attract diverse youth who will be able to meet the technical and scientific challenges awaiting the workforce of the future. To aid us in expanding our reach, we will engage our strategic partnerships with organizations help shape and promote STEM education programs. This includes educators from Girl Scouts of America (GSUSA), the National Society of Black Physicists (NSBP) and the Indigenous Education Institute (IEI). We have worked with the NASA Explorer Schools across the country, each having a majority of underserved or underrepresented students and will continue to work especially with minority-dominant schools drawing in new teachers into our CoP and introducing the SWAC program to these diverse communities in our PD efforts.

3.1 UC Berkeley Budget

Justification

It is anticipated that to complete the RHESSI SSL E/PO work on Cal Day and the Heliophysics Educator CoP will require 3% of Laura Peticolas' time per month each year and ~2 weeks of Darlene Yan's time around the time of Cal Day each year (cost for salary & benefits in budget table above.) For years FY14-15, supplies are anticipated each year at two \$600 honoraria (1 each for 2 CoP teachers each year to attend face-to-face meetings and present), teaching materials to be purchased, communications costs with teachers and coordination and Cal Day printing costs. In FY 16-18, we anticipate each year will incur similar costs as FY14-15 but budgeting only one CoP teacher honoraria each year.

3.2 Goddard Budget (in \$K)

RHESSI Goddard E/PO Budget	FY14	FY15	FY16	FY17	FY18
2. Other Direct Costs	10	10	10	10	10
a. Subcontracts	10	10	10	10	10
Hours	104	102	100	98	96
7. Total E/PO Estimated Costs	\$10	\$10	\$10	\$10	\$10

Justification

We have entered the costs in the overall budget under subcontracts since the work will be done by Elaine Lewis, the SWAC manager, under the SESDA-III contract with Adnet.

4 RHESSI LEGACY MISSION ARCHIVE PLAN

4.1 Introduction

Normal RHESSI (Lin et al. 2002) operations are largely autonomous, with a routine daily command upload containing the telemetry schedule and occasional adjustments to instrument parameters. Except during eclipse periods, passages through the South Atlantic Anomaly, and an annual Crab Nebula observing campaign, RHESSI observes the full Sun continuously.

The primary science data are returned in event data packets whose contents include the time, energy and detector-segment identification for each detected photon. Aspect data are provided with sufficient time resolution that the instantaneous aspect associated with each detected event can be inferred. Monitor Rates with lower time resolution are also available to provide an overview of detector performance.

Data acquisition averages about 2 GB per day and is based on a store-and-dump system using a 4 GB on-board memory. There are typically ~11 prescheduled downlink passes per day divided between the Berkeley Ground Station (BGS) and NASA Wallops Ground Station (WGS) with additional telemetry support provided by ground stations at Merritt Island (MILA), Weilheim, Germany, and Santiago, Chile (AGO).

Because the RHESSI data is photon-based, analysts can (iteratively) choose the optimum time, spectral and spatial resolution and coverage best suited to his/her specific science objectives and the flare(s) in question. Such decisions can therefore be made during the analysis phase, as opposed to the implementation or operations phase of the mission. This provides a powerful degree of flexibility, the value of which has been well proven over the years. Preserving this flexibility is a primary driver for the RHESSI analysis software and data strategy.

4.2 Current RHESSI Data Archive, Software and Documentation

4.2.1 RHESSI Data Archive

The current RHESSI data archive contains the full Level-0 telemetry data, the RHESSI flare list, and a number of catalog or quicklook data products (QLPs) including mission-long light curves, flare spectra and images, and summaries of housekeeping data. The full archive (~7 TB as of March 2013) resides on servers at SSL and is automatically mirrored at GSFC and the HESSI European Data Center (HEDC) at FHNW, Windisch, Switzerland. It is online and accessible by anyone with an Internet connection. The on-line archive, including metadata, quicklook products and engineering data, is updated automatically, typically within an hour of receipt at the MOC by converting the received telemetry to FITS files and adding it to the online dataset where it is available for scientific analysis.

The Level-0 data files contain the full raw telemetry data in packed time-ordered format. All of the quicklook product generation and detailed analyses of RHESSI data start with the Level-0 files. These files are in FITS format and contain science data ('photon-tagged events' that encode the detector ID, arrival time, and energy for each detector count), monitor rates, solar aspect data and housekeeping data. Even though these files are in standard FITS format, they are meaningful only through the RHESSI SSW software due to the complicated unpacking algorithms. Calibration information needed to interpret these data is distributed with and accessed by the analysis software. The entire Level-0 database is currently being backed up into a deep archive at the NSSDC with a latency of a few months. As of March 2013, it contains data through December 2012.

The QLPs include a flare list containing the time, duration, size, location, and other parameters and flags for the >70,000 events automatically identified in the RHESSI data. The full flare list is available in the archive (and viewable through a browser) as one large text file. In

addition, monthly flare list files are stored in FITS format, as well as text files for easy direct viewing. The RHESSI software reads the FITS files, automatically merging the monthly files, and provides options for selecting analysis time intervals based on flare parameters.

The QLPs allow the RHESSI observations to be surveyed. Using the same software used for higher-level analysis, they are created automatically from the Level-0 data both as FITS files and browser-viewable image formats such as GIF, PNG, or text files.

The FITS QLPs include daily observing summary data files from which analysts can quickly generate 4-second plots of light curves in 9 standard energy bands, spacecraft ephemeris, pointing and modulation variance. For most flares, the QLPs also include representative spectra and images that are intended as a starting point for most analyses. (Detailed analysis of a flare is usually done using the Level-0 data, where the user can select the times, energies, detectors, etc. that are best suited to the scientific objectives and the event under study.) The prepared plots can be viewed directly by accessing the archive metadata directories, or more easily through the versatile RHESSI Browser at <http://sprg.ssl.berkeley.edu/~tohban/browser/>. This allows users to display more than 20 different products (including light curves, images, spectra, monitor rates and comparisons with GOES, WIND/WAVES and WIND/3DP). In addition, RHESSI housekeeping data for the entire mission are available in the archive and can be accessed at http://hessi.ssl.berkeley.edu/hessidata/metadata/hsi_1day_sohdata/.

Text files and GIF plots provide a record of the average daily values for ~100 state-of-health parameters including spacecraft bus voltages and currents, imager aspect sensor parameters, spectrometer cryocooler power and temperature, and more.

Access to the data archive is almost transparent. Users located at a site hosting the full data archive (Goddard, Berkeley, or FHNW) share the data directories from a local file server. Remote users set a feature in the software to enable network searching and copying of files from an archive to their own computer. In either case, the software automatically determines the files needed for the selected time interval and after either sharing or copying them, reads them and retrieves the requested data for processing.

4.2.2 Software

Almost all the RHESSI software package (Schwartz et al. 2002) is written in Interactive Data Language (IDL, licensed from Exelis Visual Information Solutions). It contains all procedures necessary to read and unpack the FITS data files, prepare and plot light curves, reconstruct images, and accumulate, display, and analyze spectra. Analysis procedures can be invoked from a combination of the IDL command line, user-generated scripts building on these commands, or a graphical user interface (GUI) that forms a user-friendly shell around the basic analysis routines. The software is fully compatible with Linux, Mac OS X, and Windows operating systems and is freely available as part of the Solar Software (SSW) tree.

The RHESSI data analysis software is a robust object-oriented system that allows any analyst with access to Level-0 files, calibration data, and the QLPs to generate and analyze RHESSI lightcurves, spectra, and images. Higher level capabilities include generating image cubes and movies of images at multiple time and energy intervals, background subtraction, feature-based imaging spectroscopy, and performing joint analysis of many different observations of the same events by other observatories. The software can be downloaded to any user's computer as part of the Solar Software (SSW) installation following instructions provided on the RHESSI web site. The only requirement is that the user has a license for IDL Version 5.6 or higher.

4.2.3 Documentation and Support

Extensive documentation describing the mission, instrumentation, analysis techniques, software, and data access can be found via a single RHESSI web site:

<http://hesperia.gsfc.nasa.gov/rhessi/>. Support personnel at SSL and GSFC are also available to provide guidance as needed in using the software and interpreting the results.

The extensive online RHESSI documentation provides both background and explanatory material on the RHESSI mission, as well as instructions for almost every aspect of the software, from installation through use of the objects and the GUI. Detailed descriptions of every data product and warnings about misinterpreting data are available. There are 'First Steps' instructions for imaging and spectroscopy to guide users through sample GUI sessions and explanations of the use of the objects. A software FAQ is available to provide solutions to common questions or problems.

There is a dedicated email address (hessibugs@hesperia.gsfc.nasa.gov), monitored by one of the team members, for RHESSI software bug reports and questions. Queries are answered promptly either by the monitor or by core members of the RHESSI group who can be called upon as needed to address more specialized issues. All bug reports and their solutions are archived for user access.

4.3 Plans for the RHESSI Legacy Archive

4.3.1 Introduction

The legacy archive will include the data products, software, and documentation discussed above, as well as secondary databases of scientific interest and several new data products under development, all of which are described in more detail below. This section emphasizes the tasks related to adapting and enhancing those data sets to make them effective with a reduced (or eliminated) level of support from the instrument team.

4.3.2 Data Products

4.3.2.1 *Quicklook Products*

The Level-1 data products serve the needs of those requiring a convenient overview of the data and basic X-ray data products (light curves, representative images, and spectra, etc.). The catalog data to be archived for post-mission use are identical in form and content to that described in Section 4.2.

4.3.2.2 *Level-0 Data*

To meet the needs of solar and non-solar analyses without compromising the full potential of the data, the Level-0 data as described in Section 4.2 will be made part of the resident and permanent archives, along with the corresponding analysis tools and documentation.

4.3.2.3 *Visibility Data*

As discussed above, a key driver of the RHESSI analysis approach has been to maintain the ability of the user to flexibly choose the time, spatial, and energy resolution and range that best matches their scientific objectives and events under study. To achieve this, however, it is necessary for users to start from Level-0 data and use the RHESSI-specific IDL software package. While this continues to be effective, it may become more problematic without the occasional one-on-one interaction with experienced users. For the long-term, therefore, it is desirable to identify a way by which most of the flexibility can be maintained without necessarily resorting to the Level-0 data.

Visibilities provide a natural way to accomplish this. A RHESSI visibility is a fully calibrated measurement of a specific Fourier component of the source spatial distribution for a given time interval and (count) energy bin. In radio parlance, each visibility corresponds to a single uv point. Such visibilities are a direct output of RHESSI's time-modulated measurements of X-ray flux. While RHESSI's 'normal' imaging algorithms bypass the explicit calculation of visibilities,

within the last two years, the object-oriented software to convert RHESSI's photon-based data to calibrated visibilities has been incorporated into the RHESSI software package and an increasing fraction of papers now use visibility-based analyses. Furthermore, some capabilities, such as the generation of electron-images, can only be generated through visibilities. In addition to the efforts of the RHESSI PI team, the High Energy Solar Physics in Europe (HESPE) program, funded by ESA, is generating and archiving visibility-based data for long-term use.

While making some compromises in time and/or energy resolution, the use of visibilities has several distinct advantages.

- Visibilities are an inherently compact representation of the RHESSI data, preserving its key information content in a form that is typically ~ 2 orders of magnitude more compact than photon-based data.
- Unlike reconstructed images, visibilities are a *linear* representation of the data so they can be combined across different time/energy ranges to meet the user's needs.
- For each detected energy range, visibilities are fully calibrated, thus relieving the user of instrument-specific calibration tasks.
- Visibilities provide a more robust method of determining accurate source sizes as compared to inspection of reconstructed images.
- Measured visibilities include well-determined statistical errors whose propagation supports quantitative assessment of the significance of derived results.
- Calibrated X-ray visibilities have the identical significance as visibilities obtained from radio interferometers. Thus, a set of X-ray visibilities can be manipulated and converted to an image using any of several existing radio interferometer analysis packages, independent of RHESSI-specific software.

These considerations suggest that, in addition to the catalog and Level-0 data products discussed above, the inclusion of an extensive set of calibrated flare X-ray visibility data would provide a flexible option to meet the needs of users well into the future.

To do so, the following tasks remain to be accomplished:

- While the basic software for visibility calculation has been implemented, there are several important areas in which it needs to be refined.
- Automated algorithms need to be developed to optimally choose statistically significant time and energy intervals within which to calculate visibilities. Such algorithms are currently under development for other missions (e.g. Solar Orbiter) and can be re-parameterized for the present purpose.
- The suitability of FITS as the optimum archive format for the calculated visibilities to support long-term use and compatibility with radio software packages needs to be confirmed.
- Scripts need to be developed and executed to apply these algorithms to the mission-long RHESSI data set and to convert the visibilities to the archive format.
- More extensive documentation needs to be developed for use by unsupported users in the Resident and/or Permanent archive phases.

4.3.2.4 Level-2 Data Products

We are in the process of adding three science-ready event-oriented databases for photon images, spectra and lightcurves. This effort has been funded under the data environment enhancement program. The FITS files created will be readable in any scientific software environment. For each flare, we will include:

- High quality photon flux images made using the pixon algorithm in our standard energy bands at a cadence dictated by the data rates. Using about 10,000 counts per sub-collimator these images will show the principal flaring structures in the corona at low energy, and in the chromosphere at higher energy. While not suitable for imaging spectroscopy or high time-resolution studies, they will be extremely useful in correlative studies at non X-ray wavelengths and will require no further RHESSI-specific analysis.
- Photon lightcurves made in our standard energy bands up to 300 keV. These data will be background-subtracted allowing for spectral deconvolution from counts to photons. While it won't be possible to remove all instrument artifacts, these lightcurves will be suitable for immediate display and comparison with other wavelengths.
- Photon spectra up to 300 keV will be produced on a time-scale commensurate with the images produced in the nonthermal energy range. Count spectra and estimated background spectra will also be available, as well as any needed detector responses for use with our spectral analysis package

4.3.2.5 *Other RHESSI Databases*

The additional databases described in this section have the common feature that the data are distributed throughout the multi-terabyte Level-0 database. For the convenience of non-experts, we extract and process the relevant material into compact, standalone databases for subsequent analysis.

Solar Radius Data

In addition to providing essential pitch and yaw aspect data for X-ray image reconstruction, the Solar Aspect System (SAS) data constitute a unique database of highly precise measurements of solar radii (Fivian et al. 2005) with applications to fundamental solar properties such as solar oblateness and p-modes,. The dataset comprises ~100 radius measurements per second (totaling $>2 \times 10^{10}$ measurements to date), each with a statistical error of a few tens of milli-arcseconds.

SAS data require elaborate analyses to remove diverse systematic effects in order to obtain their inherent precision. As a result, these data benefit from the creation of secondary databases, both to isolate the SAS data set itself and to reflect the application of internally derived calibration parameters. Although a preliminary version of such a database exists, for the legacy archive, it will need to be finalized and fully documented, a task that will require ~ 1 man-year.

Radiation Studies

Mission-long examination of nuclear radiation data is useful for studies of galactic Al^{26} , galactic positron annihilation, novae, and quiet-Sun 2.2 MeV neutron-capture-line emission. As the mission progresses a database of accumulated 1-minute spectra from the rear detector segments is being amassed and will be added to the Permanent Archive. Documentation will be generated during the transition to the Resident Archive Phase.

Terrestrial Gamma-Ray Flashes (TGFs)

A catalog of transient events identified by an automated TGF triggering algorithm is being assembled as the mission progresses. During the Resident Archive phase, this will be finalized and documented for use as part of the Permanent Archive.

Spectrometer Status Database

We are collecting complete records of the status of the spectrometer, including detector segmentation and threshold level changes resulting from radiation damage and detector annealing. These augment the existing calibration files and will facilitate detector selection in both spectroscopy and imaging analyses.

4.3.2.6 SDO/AIA Cutout Image Database

SDO/AIA cutout image FITS files and movies are generated for every RHESSI flare observed after Sept. 2010. The cutouts are 300 arcsec squares at the highest cadence for all the AIA channels running from a few minutes before the start of the RHESSI flare through a few minutes after the end. These movies are linked from the RHESSI Browser, and the FITS files are accessible through the Synoptic Data Archive.

4.3.3 Analysis Tools for Level-0 data

The basis for all legacy archive analysis tools is the IDL-based, SSW-distributed software that has been routinely used during the mission for the creation and interpretation of scientific data products. To maintain the integrity of the software within the dynamic SSW environment we will archive a snapshot of all the elements of the SSW tree necessary for RHESSI analysis, specifically the GEN, HESSI, X-RAY, and SPEX branches. This will ensure that the software that was working at the end of mission will continue to work into the future.

With successive cycles of progressive radiation damage and annealing, the RHESSI detector response has changed during the course of the mission. To accommodate this, detector response parameters in the SSW distribution have been periodically updated so that, transparent to the user, the appropriate time-dependent calibration parameters are applied for each analysis. In preparation of the legacy archive, it will be necessary to ensure that this calibration has been updated as required to cover the full mission.

4.3.4 Documentation

While an extensive range of documentation is available via the RHESSI website, it needs to be carefully reviewed so that it can effectively serve its purpose during the Resident and Permanent Archive phases with reduced (or absent) one-on-one support. Specifically, obsolete or conflicting material needs to be identified and updated or removed, perceived gaps need to be identified and a robust stand-alone guide to the material generated. While on-going at a low level, this task will be completed during the Resident archive phase, requiring an estimated 2 - 4 months of effort by a combination of experienced RHESSI personnel. Additional emphasis will be placed on introductory material, indexing, and consolidating distributed information to provide a mission-long overview and time-ordered log of RHESSI performance.

4.3.5 Distribution

During the year after the end of the mission, RHESSI data products will continue to be accessible from servers at SSL and GSFC (and possibly through the Swiss-funded mirror site at FHNW). The archive will then be transitioned to the Resident Archive at the Solar Data Analysis Center (SDAC) at Goddard. The legacy archive will be hosted by the National Space Science Data Center (NSSDC) at Goddard.

Access of RHESSI data through the VSO involves three approaches. The first is to include the Catalog data into the VSO. This will make it possible on one hand, to display quick-look products in VSO query results, and on the other, to download pre-calculated images or image cubes for comparison with data sets from other instruments. This requires no RHESSI-specific software.

The second approach is to implement event-based queries, i.e. queries based on the flare list and the observing summary in addition to queries based on a time range. This means that the RHESSI archive can be searched, for example, for flares of specific characteristics such as size, duration, or location on the limb.

The third approach is to provide an indexed database of flare visibilities, a subset of which can be identified and provided in response to user time, energy, location or other criteria. These

can be manipulated and/or converted to images at the user's institution using either a simplified subset of IDL software or by external radio interferometric packages such as Miriad. To allow correct inclusion of the RHESSI data into the VSO, the Catalog data will be annotated in the FITS headers with keywords defined by the SPASE consortium. Adopting SPASE keywords will guarantee that SPASE data analysis programs can use RHESSI Catalog data. The visibility data will also be described by SPASE-compatible keywords. The Level-0 database, however, does not need to be SPASE annotated, as it requires the RHESSI-specific software to generate science-ready products.

4.3.6 Schedule

Estimates of the effort required to go from the end of mission to complete documentation and delivery of the legacy archive are as follows: Catalog and Level-0 data preparation: 0.1 FTE; visibility data software development, validation and database generation 2 FTE, solar radius data 1 FTE; radiation studies: 0.2 FTE; TGF database: 0.2 FTE; analysis tools, 0.2 FTE; documentation 0.4 FTE, distribution, 0.5 FTE; for a total of 4 to 5 FTE. These tasks should be completed within an elapsed time of ~2 years from the end of mission using an appropriate mix of experienced RHESSI personnel. This suggests that the cost of the final archiving effort will be in the range of \$0.8M to \$1M.

4.4 References

- Fivian, M. D., Hudson, H. S., & Lin., R. P. 2005 in *Proc 11th European Solar Physics Meeting*, ESA SP- 600, 41
- Lin, R. P., et al. 2002, *Solar Phys.*, 210, 3
- Schwartz, R. A., et al. 2002, *Solar Phys.*, 210, 165

ACRONYM LIST

A&A	Astronomy & Astrophysics Journal
AAS	American Astronomical Society
ACE	Advanced Composition Explorer
ACS	Attitude Control System
AESP	Aerospace Education Services Program
AGILE	Italian Space Agency gamma-ray mission
AGO	Santiago ground station
AGU	American Geophysical Union
AIA	Atmospheric Imaging Assembly on SDO
AIM	Aeronomy of Ice in the Mesosphere
AISES	American Indian Science and Engineer Society
ALMA	Atacama Large Millimeter/submillimeter Array
ApJ	Astrophysical Journal
ARTEMIS	Acceleration, Reconnection, Turbulence and Electrodynamics of the Moon's Interaction with the Sun
ASIM	Atmosphere-Space Interactions Monitor
ATS	Absolute Time Sequence
AU	Astronomical Unit
BATSE	Burst and Transient Source Experiment on CGRO
BBSO	Big Bear Solar Observatory
BGO	Bismuth Germinate used as a scintillation detector
BGS	Berkeley Ground Station
BPSK	Binary Phase Shift Keying
Cal Day	Open House at the Space Sciences Laboratory at the University of California, Berkeley
CAST	CERN Axion Solar Telescope
CCD	Charge Coupled Device
C&DH	Command and Data Handling
CD-ROM	Compact Disk – Read Only Memory
CDS	Coronal Diagnostic Spectrometer on SOHO
CERN	European Organization for Nuclear Research
CHIPS	Cosmic Hot Interstellar Plasma Spectrometer
CGRO	Compton Gamma Ray Observatory
CINEMA	Cubesat for Ion, Neutral, Electron, & Magnetic fields
CLI	Command Line Interface
CME	Coronal Mass Ejection
CoMP	Coronal Multi-channel Polarimeter
COMPTEL	Compton Telescope on CGRO
CoP	Community of Practice
COR-1	Inner Coronagraph of STEREO SECCHI instrument
COR-2	Outer Coronagraph of STEREO SECCHI instrument
COSPAR	COMmittee on SPACe Research
CP	Charge conjugation/Parity
CRISP	Crisp Imaging Spectro-polarimeter in Sweden
CSE@SSL	Center for Science Education at Space Sciences Laboratory
CSRH	Chinese spectro-radioheliograph
CSTA	California Science Teachers Association
DEM	Differential Emission Measure
DLR	Weilheim ground station
DST	Dunn Solar Telescope National
EGRET	Energetic Gamma Ray Experiment Telescope on CGRO
ERC	Educator Resource Center
EEPROM	Electrically Erasable Programmable Read-Only Memory
EIT	Extreme Ultraviolet Imaging Telescope on SOHO
EIS	EUV imaging spectrograph on Hinode

EOVSA	Expanded Owens Valley Solar Array
E/PO	Education and Public Outreach
ETH(Z)	Eidgenossische Technische Hochschule (Zentrum), Zurich, Switzerland
EUV	Extreme UltraViolet
EUVI	Extreme UltraViolet Imager on STEREO
EVA	Extra-Vehicular Activity
EVE	Extreme Ultraviolet Variability Experiment on SDO
EVLA	Expanded Very large Array
FAST	Fast Auroral SnapshoT
FAQ	Frequently Asked Questions
FDC	Flight Dynamics Center
Fermi	Fermi Gamma-ray Space Telescope (formerly GLAST)
FFT	Fast Fourier Transform
FHNW	Fachhochschule Nordwestschweiz - University of Applied Sciences and Arts, Northwestern Switzerland
FIP	First Ionization Potential
Firefly	NASA microsatellite for studying TGFs
FITS	Flexible Image Transport System
FORMOSAT-2	Earth Observation Satellite
FOT	Flight Operations Team
FoV	Field of View
FPI	Fabry-Perot Interferometer
FTE	Full time Equivalent
FWHM	Full Width at Half Maximum
GB	Gigabytes
GBM	Gamma-ray Burst Monitor on Fermi
GDS	Ground Data System
Ge	Germanium
GeD	Germanium Detector
GEMS	Great Explorations in Math and Science
GEONS	Geomagnetic Event Observation Network by Students
GIF	Graphics Interchange Format
GLAST	Gamma-ray Large Area Space Telescope (now Fermi)
GLE	Ground Level Event
GOES	Geostationary Operational Environmental Satellite
GRB	Gamma Ray Burst
GREGOR	Gregory-type German 1.5 m solar telescope on Tenerife
GRIS	GREGOR Infrared Spectrograph
GRS	Gamma Ray Spectrometer
GSFC	Goddard Space Flight Center
G/T	Antenna gain to noise temperature ratio
GUI	Graphical User Interface
HD	Heliophysics Division
HEA	Heliophysics Educator Ambassadors
HEAD	High Energy Astrophysics Division
HE CoP	Heliophysics Educator Community of Practice
HEDC	HESSI European Data Center
HEPAD	High Energy Proton and Alpha Particle Detector on GOES
HESPE	High Energy Solar Physics in Europe
HGO	Heliophysics Great Observatory
Hinode	Japanese solar satellite - formerly Solar-B
HMI	Helioseismic and Magnetic Imager on SDO
HP	Heliophysics
HSO	Heliophysics System Observatory
HST	Hubble Space Telescope

HXR	Hard X-ray
HXT	Hard X-ray Telescope on Yohkoh
IDL	Interactive Data Language
IDPU	Instrument Data Processing Unit
IGES	Institute for Global Environmental Strategies
IMPACT	In-situ Measurements of Particles and CME Transients on STEREO
IPM	Interplanetary Medium
IPN	Interplanetary Network
ISSI	International Space Science Institute
ISUAL	Imager of Sprites and Upper Atmospheric Lightnings on FORMOSAT-2
ITOS	Integrated Test and Operations System
JGR	Journal of Geophysical Research
KSC	Kennedy Space Center
LASCO	Large Angle and Spectrometric Coronagraph on SOHO
LAT	Large Area Telescope on Fermi
LDGRF	Long Duration Gamma-Ray Flares
LHCP	Left-Handed Circular Polarization
LHS	Lawrence Hall of Science
LSEP	Large SEP event
mas	milli-arcsecond
MB	Megabytes
MDI	Michelson Doppler Imager on SOHO
MHD	Magnetohydrodynamics
MILA	Merritt Island ground station
MOC	Mission Operations Center
MO&DA	Mission Operations and Data Analysis
MOU	Memorandum of Understanding
MPS	Mission Planning System
NaI	Sodium Iodide used as a scintillation particle detector
NASA	National Aeronautics and Space Administration
NCAR	National Center for Atmospheric Research
NRH	Nancay Radioheliograph
NSO	National Solar Observatory
NSSDC	National Space Science Data Center
NSTA	National Science Teacher Association
NuSTAR	Nuclear Spectroscopic Telescope Array - orbiting telescopes to focus HXRs
OCA	Orbital Carrier Aircraft
OEPM	NASA's Office of Education Performance Measurement
OIG	Orbital Information Group
OVSA	Owens Valley Solar Array
PD	Professional Development
PMTRAS	Photomultiplier Tube Roll Angle System
PNG	Portable Network Graphics
POEMAS	POLarization Emission of Millimeter Activity at the Sun in Argentina Polarimetric Littrow Spectrograph
PSG	Prioritized Science Goals
PSLA	Project Service Level Agreement
QLP	Quick Look data Product
RAD6000	Radiation-hardened single board computer used on spacecraft
RAID	Redundant Array of Inexpensive Disks
RAS	Roll Angle System
RF	Radio Frequency
RHCP	Right-Handed Circular Polarization
RHESSI	Reuven Ramaty High Energy Solar Spectroscopic Imager
RMC	Rotating Modulation Collimator
SAA	South Atlantic Anomaly

SACNAS	Society for Advancement of Chicanos and Native Americans in Science
SAMPEX	Solar Anomalous and Magnetospheric Particle Explorer
SAS	Solar Aspect System
SatTrack	Satellite Tracking software
SDAC	Solar Data Analysis Center
SDO	Solar Dynamics Observatory
SECCHI	Sun Earth Connection Coronal and Heliospheric Investigation on STEREO
SECEF	Sun Earth Connection Education Forum
SED	Sun-Earth Day
SEE	Solar Eruptive Event
SEGway	Science Education Gateway
SEP	Solar Energetic Particles
SEPT	Solar Electron Proton Telescope on STEREO / IMPACT
SERS	Spacecraft Emergency Response System
SHH	Soft, Hard, Harder –HXR spectral evolution
SHS	Soft, Hard, Soft – HXR spectral evolution
SMD	Science Mission Directorate
SMEX	NASA's Small Explorer Program
SMM	Solar Maximum Mission
SOC	Science Operations Center
SOH	State-Of-Health
SOHO	Solar and Heliophysics Observatory
SORCE	Solar Radiation and Climate Experiment
SOT	Solar Optical Telescope on Hinode
SOXS	Solar X-ray Spectrometer
SPASE	Space Physics Archive Search and Extract
SPD	Solar Physics Division
SSL	Space Sciences Laboratory (University of California, Berkeley)
SSMO	Space Science Mission Operations
SSR	Solid State Recorder
SSRT	Siberian Solar Radio Telescope
SST	Swedish Solar Telescope
SSW	SolarSoftware
STE	Suprathermal Electron Telescope on STEREO / IMPACT
STEM	Science, Technology, Engineering, and Math
STEREO	Solar TErestrial RElations Observatory
STIX	Spectrometer Telescope for Imaging X-rays
SWAC	Space Weather Action Center
SXI	Soft X-ray Imager
SXR	Soft X-ray
TARANIS	Tool for the Analysis of RAdiations from lightNings and Sprites
TB	Terabytes
TGF	Terrestrial Gamma-ray Flash
THEMIS	Time History of Events and Macroscale Interactions during Substorms
TRACE	Transition Region and Coronal Explorer
UCB	University of California at Berkeley
UT	Universal Time
VCn	Virtual Channel n
VSO	Virtual Solar Observatory
VxWorks	A real-time operating system
WAVES	Radio and Plasma Wave Investigation on the WIND spacecraft
WebEx	Web conferencing application
WGS	Wallops Ground Station
WIND	Spacecraft for long-term solar wind measurements
WISE	Wide Field Infrared Survey Explorer
WLF	White-Light Flare

WWLLN	World Wide Lightning Location Network
WYE	Work Year Estimate
XRT	X-Ray Telescope on Hinode
Yohkoh	Japanese Solar Satellite